

UNCLASSIFIED

AD NUMBER	
AD384742	
CLASSIFICATION CHANGES	
TO:	UNCLASSIFIED
FROM:	SECRET
LIMITATION CHANGES	
TO: Approved for public release; distribution is unlimited.	
FROM: Distribution authorized to U.S. Gov't. agencies only; Administrative/Operational Use; OCT 1967. Other requests shall be referred to Aeronautical Systems Div., Wright-Patterson AFB, oh 45433.	
AUTHORITY	
ASD ltr 1 Dec 1972; ASD ltr 16 Aug 1977	

THIS PAGE IS UNCLASSIFIED

300427  
AEDC-TR-67-213

DECLASSIFIED / UNCLASSIFIED

~~SECRET~~  
**ARCHIVE COPY  
DO NOT LOAN**

ARO, INC.  
DOCUMENT CONTROL  
NO 1G-677-343  
COPY 1 OF 43  
SERIES A PAGES 76



300427  
**WIND TUNNEL INVESTIGATION OF A 0.10-SCALE  
NORTH AMERICAN AVIATION AMSA INLET AT TRANSONIC  
AND SUPERSONIC MACH NUMBERS (U)**

H. E. McDill and J. F. Riddell

ARO, Inc.

October 1967

Approved for public release; distribution unlimited.

In addition to security requirements which apply to:

Pub Release

JAN 1968  
JUN 1968  
JUN 1969  
JUN 1970  
JUN 1971  
JUL 1972

Distribution limited to U. S. Gov't Agencies only; Test and evaluation; Nov. 72. Other requests for this document must be referred to Commander, Aeronautical Systems Div., Attn: VHL, Wright-Patterson AFB, Ohio 45433. Per TAB T3-2, dated 15 Jan. 73.

CLASSIFICATION CANCELLED  
BY AUTHORITY OF *Alfred Memo #812/10-72*  
BY *E. H. Boyd*  
Name and Position of individual  
Date *8 Dec 72*

**PROPULSION WIND TUNNEL FACILITY  
ARNOLD ENGINEERING DEVELOPMENT CENTER  
AIR FORCE SYSTEMS COMMAND**

**ARNOLD AIR FORCE STATION, TENNESSEE**

DECLASSIFIED / UNCLASSIFIED

PROPERTY OF U. S. AIR FORCE  
AEDC LIBRARY  
AF 40(600)1200

GROUP 3  
Downgraded at 12 year intervals;  
Not automatically declassified.  
DOD DIR 5200.10

AEDC TECHNICAL LIBRARY

5 0720 00031 6010

~~SECRET~~

# ***NOTICES***

When U. S. Government drawings specifications, or other data are used for any purpose other than a definitely related Government procurement operation, the Government thereby incurs no responsibility nor any obligation whatsoever, and the fact that the Government may have formulated, furnished, or in any way supplied the said drawings, specifications, or other data, is not to be regarded by implication or otherwise, or in any manner licensing the holder or any other person or corporation, or conveying any rights or permission to manufacture, use, or sell any patented invention that may in any way be related thereto.

Qualified users may obtain copies of this report from the Defense Documentation Center.

References to named commercial products in this report are not to be considered in any sense as an endorsement of the product by the United States Air Force or the Government.

Do not return this copy. When not needed, destroy in accordance with pertinent security regulations.

~~SECRET~~

AEDC-TR-67-213

DECLASSIFIED / UNCLASSIFIED

WIND TUNNEL INVESTIGATION OF A 0.10-SCALE  
NORTH AMERICAN AVIATION AMSA INLET AT TRANSONIC  
AND SUPERSONIC MACH NUMBERS (U)

Distribution limited to U. S. Government only; Test and Evaluation requests for this document must be referred to Commanding Aeronautical Systems Div., Attn: [redacted] Wright-Patterson AFB, Ohio 45433. Per TAB 73-2, dated 15 Jan. 73.

H. E. McDill and J. F. Riddell  
ARO, Inc.

Approved for public release; distribution unlimited.

In addition to security requirements which apply to this document and must be observed by each transmittal outside the Department of Defense must have prior approval of the Aeronautical Systems Division (ASD), Wright-Patterson AFB, Ohio.

In addition to security requirements which must be met, this document is subject to special export controls and each transmittal to foreign governments or foreign nationals must be made only with prior approval of the Aeronautical Systems Division (ASD), Wright-Patterson AFB, Ohio.

This material contains information affecting the national defense of the United States within the meaning of the Espionage Laws (Title 18, U.S.C., sections 793 and 794) the transmission or revelation of which in any manner to an unauthorized person is prohibited by law.

CLASSIFICATION CANCELLED (CHANGED TO UNCLASSIFIED)  
BY ACTION OF ASD Tech Memo #812, 1 Dec 72  
BY [redacted] 2 Dec 72  
Name and position of individual Date

DECLASSIFIED / UNCLASSIFIED

~~SECRET~~

This page is Unclassified

~~SECRET~~

DECLASSIFIED / UNCLASSIFIED

## FOREWORD

(Unclassified) The work reported herein was done at the request of the Aeronautical Systems Division (ASD) (ASZD), Air Force Systems Command (AFSC), for North American Aviation, Inc. under Program Element 6340683F, System 139A.

(Unclassified) The results of the test presented were obtained by ARO, Inc. (a subsidiary of Sverdrup & Parcel and Associates, Inc.), contract operator of the Arnold Engineering Development Center (AEDC), AFSC, Arnold Air Force Station, Tennessee, under Contract AF40(600)-1200. The test was conducted from May 2 through 10, 1967 and June 2 through 24, 1967 under ARO Project No. PT0744, and the manuscript was submitted for publication on September 12, 1967.

(Unclassified) This report contains classified information extracted from North American Aviation's reports NA-66-1354 dated 3-2-67, Secret, Group 3, and report TFD-67-402 dated April 1967, Secret, Group 3.


(Unclassified) This technical report has been reviewed and is approved.

Richard W. Bradley  
Lt Col, USAF  
AF Representative, PWT  
Directorate of Test

Leonard T. Glaser  
Colonel, USAF  
Director of Test

DECLASSIFIED / UNCLASSIFIED

11

  
This page is Unclassified

**DECLASSIFIED / UNCLASSIFIED**

**SECRET ABSTRACT**

(Secret) Test results are presented for a study on a 0.10-scale model of the North American Aviation proposed advanced manned strategic aircraft air vehicle. Inlets of various geometries were tested at Mach numbers from 0.60 to 2.20 over an angle-of-attack range from 0.2 to 13 deg and angles of yaw from -5.0 to +5.0 deg. Inlet performance in terms of compressor-face total-pressure recovery and flow distortion is presented as a function of mass-flow ratio for various inlet geometries at several Mach numbers and model attitudes.

~~Approved for public release; distribution unlimited.~~

In addition to security requirements which apply to this document and must be met, each transmittal outside the Department of Defense must have prior approval of Aeronautical Systems Division (ASD), Wright-Patterson AFB, Ohio.

In addition to security requirements which must be met, this document is subject to special export controls and each transmittal to foreign governments or foreign nationals may be made only with prior approval of Aeronautical Systems Division (ASD), Wright-Patterson AFB, Ohio.

Distribution limited to U. S. Government agencies only; Test and Evaluation: 1. 2. Other requests for this document must be referred to Commander, Aeronautical Systems Div., Attn: [redacted] Wright-Patterson AFB, Ohio 4542. Per TAB 73-2, dated 15 Jan. 73.

**DECLASSIFIED / UNCLASSIFIED**

## CONTENTS

	<u>Page</u>
ABSTRACT . . . . .	iii
NOMENCLATURE . . . . .	viii
I. INTRODUCTION . . . . .	1
II. APPARATUS	
2.1 Test Facility . . . . .	1
2.2 Test Article . . . . .	1
2.3 Instrumentation . . . . .	2
III. PROCEDURE . . . . .	3
IV. RESULTS AND DISCUSSION	
4.1 Boundary-Layer Thickness in the Inlet Flow Field . . . . .	4
4.2 Initial Boundary-Layer Control Development . . . . .	4
4.3 Subsonic Diffuser Selection . . . . .	6
4.4 Performance Improvement . . . . .	6
4.5 Effect of Mach Number on Inlet Performance . . . . .	7
4.6 Effect of Angle of Attack on Inlet Performance . . . . .	8
4.7 Effect of Yaw Angle on Inlet Performance . . . . .	9
4.8 Effect of Throat Height on Inlet Performance . . . . .	11
4.9 Effect of Bypass on Inlet Performance . . . . .	11
V. CONCLUSIONS . . . . .	12
REFERENCES . . . . .	13

## APPENDIXES

### I. ILLUSTRATIONS

#### Figure

1. (Unclassified) Model Location in the Test Section	
a. Tunnel 16S . . . . .	17
b. Tunnel 16T . . . . .	18
2. (Unclassified) Model Installation	
a. Tunnel 16S . . . . .	19
b. Tunnel 16T . . . . .	20
3. (Unclassified) Boundary-Layer Control Configurations	
a. Porous Plate Locations and Percent Porosity . . . . .	21
b. Boundary-Layer Gutters and Porous Plate Installation on Ramp and Upper Sideplate . . . . .	22
4. (Unclassified) Bypass System Configuration . . . . .	23

~~SECRET~~  
DECLASSIFIED / UNCLASSIFIED

<u>Figure</u>	<u>Page</u>
5. (Unclassified) Fuselage and Wing Boundary-Rakes . . . . .	24
6. (Unclassified) Photograph of Inlet Boundary-Layer Rakes . . . . .	25
7. (Unclassified) Compressor-Face Instrumentation . . . . .	26
8. (Unclassified) ASME Nozzles M1 and M2 Instrumentation . . . . .	27
9. (Unclassified) Duct Pressure Instrumentation . . . . .	28
10. (Unclassified) Summary of Test Conditions . . . . .	29
11. ( <del>Secret</del> ) Fuselage and Wing Boundary-Layer Total-Pressure Profiles at $M_\infty = 2.20$	
a. $\alpha = 0.2$ deg . . . . .	30
b. $\alpha = 4.0$ deg . . . . .	31
c. $\alpha = 11.0$ deg. . . . .	32
12. ( <del>Secret</del> ) Variation in Total-Pressure Recovery as a Function of Throat Height for BLC Configurations J2 and J4, $M_\infty = 2.20$ , $\alpha = 4.0$ deg, $\psi = 0$ deg. . . . .	33
13. ( <del>Secret</del> ) Inlet Performance of BLC Configurations J2 and J4 as a Function of Mass-Flow Ratio, $M_\infty = 2.20$ , $\alpha = 4.0$ deg, $\psi = 0$ deg . . . . .	34
14. (Unclassified) Subsonic Diffuser Area Distribution . . . . .	35
15. ( <del>Secret</del> ) Variation in Total-Pressure Recovery as a Function of Throat Height for Subsonic Diffusers A and D, $M_\infty = 2.20$ , $\alpha = 4.0$ deg, $\psi = 0$ deg . . . . .	36
16. ( <del>Secret</del> ) Inlet Performance of Subsonic Diffusers A and D as a Function of Mass-Flow Ratio, $M_\infty = 2.20$ , $\alpha = 4.0$ deg, $\psi = 0$ deg, TH = 110 percent T-L . . . . .	37
17. (Unclassified) Location of Vortex Generators	
a. Cowl Surface . . . . .	38
b. Ramp Surface . . . . .	39
18. ( <del>Secret</del> ) Effect of Vortex Generator Location on Inlet Performance, $M_\infty = 2.20$ , $\alpha = 4.0$ deg, $\psi = 0$ deg, TH = 104 percent T-L . . . . .	40
19. ( <del>Secret</del> ) Variation in Total-Pressure Recovery as a Function of Throat Height for Model Configurations 7, 14, and 19, $M_\infty = 2.20$ , $\alpha = 4.0$ deg, $\psi = 0$ deg. . . . .	41

~~SECRET~~

<u>Figure</u>		<u>Page</u>
20.	( <del>Secret</del> ) Inlet Performance of Model Configurations 7, 14, and 19 as a Function of Total Engine Mass-Flow Ratio, $M_\infty = 2.20$ , $\alpha = 4.0$ deg, $\psi = 0$ deg, TH = 110 percent T-L . . . . .	42
21.	( <del>Secret</del> ) Effect of Mach Number on Inlet Performance, $\alpha = 4.0$ deg, $\psi = 0$ deg	
	a. $M_\infty = 0.60$ , Configuration 22 . . . . .	43
	b. $M_\infty = 0.85$ , Configuration 22 . . . . .	44
	c. $M_\infty = 1.20$ , Configuration 22 . . . . .	45
	d. $M_\infty = 1.50$ , Configuration 27 . . . . .	46
	e. $M_\infty = 1.75$ , Configuration 19 . . . . .	47
	f. $M_\infty = 2.00$ , Configuration 19 . . . . .	47
	g. $M_\infty = 2.20$ , Configuration 19 . . . . .	47
22.	( <del>Secret</del> ) Effect of Angle of Attack on Inlet Performance, $\psi = 0$ deg	
	a. $M_\infty = 0.60$ , Configuration 22 . . . . .	48
	b. $M_\infty = 0.95$ , Configuration 22 . . . . .	49
	c. $M_\infty = 1.50$ , Configuration 27 . . . . .	50
	d. $M_\infty = 2.00$ , Configuration 19 . . . . .	51
	e. $M_\infty = 2.20$ , Configuration 19 . . . . .	51
23.	( <del>Secret</del> ) Effect of Yaw on Inlet Performance, $\alpha = 4.0$ deg, $\psi = -5.0$ to $+5.0$ deg	
	a. $M_\infty = 0.60$ , Configuration 22 . . . . .	52
	b. $M_\infty = 0.95$ , Configuration 22 . . . . .	53
	c. $M_\infty = 1.50$ , Configuration 27 . . . . .	54
	d. $M_\infty = 2.00$ , Configuration 19 . . . . .	55
	e. $M_\infty = 2.20$ , Configuration 19 . . . . .	55
24.	( <del>Secret</del> ) Variation of Total-Pressure Recovery as a Function of Throat Height, $M_\infty = 2.20$ , $\alpha = 4.0$ deg, $\psi = 0$ deg, Configuration 19 . . . . .	56
25.	( <del>Secret</del> ) Effect of Throat Height on Inlet Performance, $\alpha = 4.0$ deg, $\psi = 0$ deg, Configuration 19	
	a. $M_\infty = 2.20$ . . . . .	57
	b. $M_\infty = 1.75$ . . . . .	58
26.	( <del>Secret</del> ) Effect of Bypass Configuration on Inlet Performance, $M_\infty = 2.20$ , $\alpha = 4.0$ deg, $\psi = 0$ deg	
	a. Bypass Configuration U1 . . . . .	59
	b. Bypass Configuration U3 . . . . .	59
	c. Bypass Configuration U2 . . . . .	60

~~SECRET~~

~~SECRET~~

DECLASSIFIED / UNCLASSIFIED

Page

## II. TABLE

I. Configuration Description . . . . . 61

III. THE INFLUENCE OF MODEL SUPPORT STRUCTURE  
ON THE FLOW ANGULARITY AND LOCAL MACH  
NUMBER AT TRANSONIC MACH NUMBERS . . . . . 62

## NOMENCLATURE

BLC	Boundary-layer airflow bleed control (Unclassified)
$D_2$	Compressor-face total-pressure distortion of each engine, $\frac{(p_{t2})_{\max} - (p_{t2})_{\min}}{(p_{t2})_{\text{avg}}}$ (Unclassified)
M	Mach number (Unclassified)
$\Delta M$	Mach number differential ( $M_L - M_\infty$ is positive for $M_\infty < M_L$ ) (Unclassified)
$M_\infty$	Uncorrected free-stream Mach number (Unclassified)
MS	Model fuselage station, in. (Unclassified)
$m_2/m_\infty$	Mass flow ratio: ratio of compressor-face station mass flow to inlet capture mass flow (capture area = 0.146317 ft <sup>2</sup> ) ( <del>Secret</del> )
$m_{2t}/m_\infty$	Total engine mass-flow ratio, $(m_2/m_\infty)_I + (m_2/m_\infty)_O$ (Unclassified)
$N_2$	Area weighted compressor-face total-pressure recovery, $(p_{t2})_{\text{avg}}/p_{t_\infty}$ (Unclassified)
$N_{2(\text{avg})}$	Average compressor face total-pressure recovery, $\frac{N_{2,I} + N_{2,O}}{2}$ (Unclassified)
p	Static pressure, psfa (Unclassified)
$p_t$	Total pressure, psfa (Unclassified)

DECLASSIFIED / UNCLASSIFIED

~~SECRET~~

$(p_{t2})_{avg}$	Area weighted average total pressure (measured at an engine face, each pressure assigned equal area), $\frac{\sum p_{t2}}{\text{number of good pressures}}$ (Unclassified)
Re	Reynolds number per foot (Unclassified)
TH	Throat height, in. (Unclassified)
T-L	Throat height at which the inlet unstarts at each Mach number and model attitude, in. (Unclassified)
VG	Vortex generators (Unclassified)
$X_{BP}$	Position of bypass flowmetering plug measured from a reference point (closed position), in. (Unclassified)
$\alpha$	Uncorrected angle of attack of wing chord line, deg (Unclassified)
$\Delta\alpha$	Angle-of-attack correction due to model support influence and tunnel flow misalignment (Unclassified)
$\gamma_{BP}$	External bypass door position, deg (Unclassified)
$\psi$	Uncorrected angle of yaw, deg (Unclassified)
$\Delta\psi$	Angle-of-yaw correction due to model support influence and tunnel flow misalignment (Unclassified)

## SUBSCRIPTS

2	Engine compressor-face location (Unclassified)
avg	Average (Unclassified)
I	Inboard (Unclassified)
L	Local conditions (Unclassified)
max	Maximum (Unclassified)
min	Minimum (Unclassified)
O	Outboard (Unclassified)
$\infty$	Free-stream conditions (Unclassified)

DECLASSIFIED / UNCLASSIFIED

This page is Unclassified

~~SECRET~~MODEL NOMENCLATURE **DECLASSIFIED / UNCLASSIFIED**

<u>Symbol</u>	<u>Description</u>
B1	Basic AMSA fuselage extending to 6 in. aft of the cowl leading edge (Unclassified)
FG1	Fuselage-inlet boundary-layer gutter height of 0.53 in. ( <del>Secret</del> )
FG2	Fuselage-inlet boundary-layer gutter height of 1.03 in. ( <del>Secret</del> )
I1	Inlet duct: variable geometry supersonic diffuser used with subsonic diffuser A (see Fig. 9) (Unclassified)
I2	Inlet duct: variable geometry supersonic diffuser used with subsonic diffuser D (see Fig. 9) (Unclassified)
I3	Inlet duct: variable geometry supersonic diffuser used with subsonic diffuser F (see Fig. 9) (Unclassified)
I4	Inlet duct: variable geometry supersonic diffuser used with subsonic diffuser G (see Fig. 9) (Unclassified)
J	Porous configuration for boundary-layer control bleed regions (see Fig. 3) (Unclassified)
LO	Inlet duct cowl: fixed cowl (Unclassified)
L1	Inlet duct cowl: variable deflection cowl (Unclassified)
M1	Metering section for main duct: includes metering approach section, nozzle and variable plug. Small nozzle: $D_I = 4.250$ in. and $D_O = 4.200$ in. ( <del>Secret</del> )
M2	Metering section for main duct: includes metering approach section, nozzle, and variable plug. Large nozzle: $D_I$ and $D_O = 5.25$ in. ( <del>Secret</del> )
UO	Bypass: no bypass (Unclassified)
U1	Bypass: bypass extending from MS 119 to MS 122 with controlled exit door ( <del>Secret</del> )
U2	Bypass: bypass extending from MS 119 to MS 122; upper half of perimeter is 51 percent porous ( <del>Secret</del> )
U3	Bypass: bypass extending from MS 119 to MS 122; entire perimeter is 51 percent porous ( <del>Secret</del> )
VO	Vortex generator configuration: no vortex generators (Unclassified)

**DECLASSIFIED / UNCLASSIFIED**~~SECRET~~

**DECLASSIFIED / UNCLASSIFIED**

- V5 Vortex generator configuration: vortex generators installed in forward location (Unclassified)
- V6 Vortex generator configuration: vortex generators installed in aft location (Unclassified)
- V7 Vortex generator configuration: vortex generators installed in middle location (Unclassified)
- W1 Wing: stub wing clipped outboard from the estimated region of wing influence (Unclassified)
- WG1 Wing-inlet boundary-layer gutter height of 0.25 in. (~~Secret~~)

**DECLASSIFIED / UNCLASSIFIED**

**DECLASSIFIED / UNCLASSIFIED****SECTION I  
INTRODUCTION**

(Unclassified) A test was conducted for North American Aviation, Inc. (NAA) on a 0.10-scale inlet model of the NAA study for a proposed advanced manned strategic aircraft (AMSA) air vehicle. The test was conducted in the Propulsion Wind Tunnels, Supersonic (16S) and Transonic (16T) of the Propulsion Wind Tunnel Facility (PWT).

(~~Secret~~) The purpose of the test was to provide data which will define the performance and operating characteristics of a mixed-compression fuselage-mounted inlet proposed by NAA for the AMSA vehicle.

(Unclassified) Test data presented in this report are the significant inlet performance characteristics of the model configurations tested. All data from this test have been provided North American Aviation, Inc.

**SECTION II  
APPARATUS****2.1 TEST FACILITY**

(Unclassified) Tunnels 16T and 16S are closed-circuit, continuous flow tunnels which are capable of operating in the Mach number range from 0.5 through 1.6 and 1.7 through 3.1, respectively. A more complete description of their operating characteristics is presented in Ref. 1. The axial location of the 0.10-scale AMSA inlet model and model support system in the tunnel test sections are shown in Figs. 1a and b (Appendix I) for 16S and 16T, respectively.

**2.2 TEST ARTICLE**

(~~Secret~~) The inlet model is a 0.10-scale replica of forward portions of the external fuselage and internal duct lines of an NAA proposed AMSA air vehicle. Externally, the fuselage lines are duplicated to a point 6 in. (model scale) aft of the cowl lip, and wing lines are duplicated with a stub left-hand wing in the region of wing-inlet influence. The internal lines are duplicated from the inlet to the engine face station for the one half of the air induction system (left-hand duct). The test model installed in Tunnels 16S and 16T test sections is shown in Fig. 2.

~~SECRET~~

DECLASSIFIED / UNCLASSIFIED

(~~Secret~~) The model is capable of remote actuation in pitch and yaw. The model throat height, cowl position, bypass plug valve position, bypass door position, and inboard and outboard plug valve position are remotely variable. The inlet consists of one fixed external ramp (first) and three movable ramps (Fig. 3) with the required linkage for actuation. The first ramp is fixed at an angle of 5 deg with respect to the centerline of the air vehicle.

(~~Secret~~) The air entering the inlet passes through the variable geometry supersonic diffuser and the subsonic diffuser to the two engine simulators. Each inlet supplies the required airflow for two engines. Duct pressure recovery is measured at each engine-face station, and the airflow through each is measured with a standard ASME nozzle and regulated with a flow control plug. The boundary-layer control (BLC) system consists of variable porosity walls in the supersonic diffuser and bleed gutters forward of the inlet. Porous and solid plates on the internal surfaces of the ramps, cowl, and upper and lower side plates are used for boundary-layer bleed. The locations of the removable plates are shown in Fig. 3a. The porosity of each bleed pattern tested is also shown in Fig. 3a. The fuselage and wing boundary-layer gutters (Fig. 3b) captured the boundary-layer approaching the inlet, and the height could be adjusted manually. Three bypass configurations were tested: one had a controlled exit door and two had porous diffusers with an exit flow control plug. A sketch of the bypass configurations is shown in Fig. 4. More details of the test model are contained in Ref. 2. Model configurations tested are listed in Table I (Appendix II).

## 2.3 INSTRUMENTATION

(~~Secret~~) The fuselage boundary-layer total-pressure profiles were determined from total-pressure measurements obtained from two rakes located 1.667 in. forward of the splitter leading edge (Figs. 5 and 6). The wing boundary-layer total-pressure profiles were also determined from total-pressure measurements obtained from two rakes located 1.63 in. forward of the upper splitter leading edge.

(Unclassified) Six 5-tube engine compressor-face rakes (Fig. 7) measured the total pressure for each engine from which the compressor-face total-pressure recovery and distortion were determined. These total-pressure orifice locations were on equal areas.

(Unclassified) The airflow of each engine simulator was metered using ASME nozzles M1 and M2 with four static taps at the nozzle throat and four static taps upstream of the nozzle (Fig. 8).

~~SECRET~~

DECLASSIFIED / UNCLASSIFIED

**DECLASSIFIED / UNCLASSIFIED**

(Unclassified) Steady-state pressure instrumentation also included static-pressure taps through the duct and various total-pressure probes within the duct (Fig. 9). In addition, there were 12 transducers mounted on the model to measure transient pressures which were recorded on oscillographs and magnetic tape.

**SECTION III  
PROCEDURE**

(~~Secret~~) The tunnel flexible-nozzle contour and pressure ratio were set to produce the desired free-stream Mach numbers. Figure 10 shows the Reynolds number and free-stream total pressures as a function of Mach number. The model angle-of-attack settings ranged from 0.2 to +13 deg and angles of yaw  $\pm 5$  deg.

(~~Secret~~) After the tunnel free-stream total pressure and Mach number were established, the model was positioned to the desired angle of attack and/or angle of yaw. At each test condition, inlet pressure data were obtained for a range of simulated engine mass flows for several throat heights. The engine(s) airflow control plugs were varied to cover a range of airflows from either engine locked rotor or the inlet buzz limit mass flow to the mass-flow ratio approaching supercritical inlet operation. Buzz was determined by monitoring the output of a pressure transducer mounted on the hub of the engine.

**SECTION IV  
RESULTS AND DISCUSSION**

(~~Secret~~) Test results are presented for a 0.10-scale inlet model of the North American Aviation AMSA air vehicle for free-stream Mach numbers from 0.6 to 2.20. The fuselage and wing boundary-layer profiles are shown for various model attitudes at  $M_\infty = 2.20$ . Inlet performance in terms of compressor-face total-pressure recovery and flow distortion is presented as a function of engine mass-flow ratio for various model configurations and model attitudes. The engine airflow requirements used are for maximum-power, standard-day operation above the tropopause and were obtained from Ref. 3. A list of the configurations tested is shown in Table I.

(Unclassified) Because the inlet was in such close proximity to the structure housing the yaw mechanism, as shown in Fig. 2b, an

**DECLASSIFIED / UNCLASSIFIED**

investigation was conducted in 16T subsequent to the inlet test to determine the magnitude of this influence on flow angularity and local Mach number at the model inlet station. The results of this investigation are presented in Appendix III. Corrections based on these results have not been applied in this report.

#### 4.1 BOUNDARY-LAYER THICKNESS IN THE INLET FLOW FIELD

(~~Secret~~) The fuselage and wing boundary-layer thicknesses in the inlet flow field were determined to adjust the boundary-layer gutter-height dimensions for the model. Thus, the gutter-height dimensions position the inlet relative to the fuselage and wing. The initial gutter heights for the fuselage and wing were set at 0.53 and 0.25 in., respectively. The total-pressure rakes used to measure the boundary-layer thickness are shown in Figs. 5 and 6.

(~~Secret~~) The measured fuselage and wing boundary-layer profiles are shown in Fig. 11 for three angles of yaw at angles of attack from 0.2 to 11.0 deg. The theoretical turbulent boundary-layer thickness for a flat plate is also shown as a dashed line.

(~~Secret~~) The measured fuselage boundary-layer thickness agrees very well with the theoretical at all combinations of positive yaw angles and angles of attack. However, at negative yaw angles the boundary layer thickens considerably on the fuselage and tends to separate from the fuselage at an angle of attack of 11.0 deg.

(~~Secret~~) The measured boundary-layer thickness on the wing surface shows close agreement with the theoretical at all yaw angles and all angles of attack except 0.2 deg where the measured value is thicker than the calculated.

(~~Secret~~) After the initial run the boundary-layer rakes were removed and the fuselage gutter height was adjusted to 1.03 in. The wing gutter height was not changed from the initial height of 0.25 in.

#### 4.2 INITIAL BOUNDARY-LAYER CONTROL DEVELOPMENT

(~~Secret~~) Three porous-wall configurations (J1, J3, and J4) and one solid-wall configuration (J2) were initially tested to select a porous-wall configuration. The throat height was set at 102, 104, 106, 110, and 116 percent of the unstart throat height (percent T-L). For

**DECLASSIFIED / UNCLASSIFIED**

**DECLASSIFIED / UNCLASSIFIED**

each of the throat height settings, the primary duct flow plugs were throttled to set the maximum engine-face total-pressure recovery which occurs just prior to an inlet unstart. The variation of the average engine-face peak total-pressure recovery as a function of the throat height is shown in Fig. 12 for the inlet with solid-plate surfaces and with selected porous-plate surfaces, bleed patterns J2 and J4, respectively. At the test conditions shown ( $M_\infty = 2.20$ ,  $\alpha = 4.0$  deg, and  $\psi = 0$  deg), the maximum pressure recovery is essentially constant for throat heights from 104 percent T-L to 110 percent T-L for the porous-plate configurations, whereas the total-pressure recovery for the solid-plate configuration is a maximum at 102 percent T-L and decreases with increasing throat height.

~~(Secret)~~ The variation of average engine-face total-pressure recovery and distortion as functions of total engine-mass-flow ratio is shown in Fig. 13. The data shown are for throat height settings corresponding to the 102 percent T-L and 110 percent T-L as noted above. For the solid-plate configuration 2 (no boundary-layer bleed flow), the maximum total-pressure recovery attainable was 0.713. Opening the flow plug (increasing corrected airflow) had the effect of moving the duct shock downstream in the diffuser while maintaining an essentially constant mass-flow ratio. As seen in Fig. 13, the total mass-flow ratio obtained with the solid-plate configuration agrees well with the theoretical predicted value of 1.055 from Ref. 3.

~~(Secret)~~ With the porous-plate configuration 6, a variation of approximately 5.0 percent in mass-flow ratio was obtained as the duct shock moved downstream in the diffuser. When the shock reached the solid surfaces (past the influence of the porous plates), the pressure recovery decreased rapidly, and further variation in the primary plug position had no significant effect on mass-flow ratio. The maximum average engine face total-pressure recovery was 0.912 at a mass-flow ratio of 0.906 and decreased as the duct shock moved downstream through the region of the porous plates. At peak total-pressure recovery the maximum bleed-mass-flow ratio was approximately 0.15.

~~(Secret)~~ The minimum value of engine-face total-pressure distortion for the solid-plate configuration was 0.22, which occurred at the outboard engine-face location, whereas the distortion for the porous-plate configuration at a mass-flow ratio of 0.915 was 0.052 and 0.040 at the inboard and outboard engine-face locations, respectively.

**DECLASSIFIED / UNCLASSIFIED**

~~SECRET~~**DECLASSIFIED / UNCLASSIFIED**

### 4.3 SUBSONIC DIFFUSER SELECTION

~~(Secret)~~ Four subsonic diffuser configurations were tested with the J4 boundary-layer bleed pattern selected above in order to determine the diffuser with the best pressure recovery and distortion characteristics. These subsonic diffusers had different diffusion rates and different local angles. The inboard and outboard wall lines and area distribution are shown in Figs. 9 and 14 versus model station, respectively.

~~(Secret)~~ The variation of average engine-face total-pressure recovery as a function of the throat height is shown in Fig. 15 for the inlet with subsonic diffusers A and D. Only performance on configurations A and D are shown since they exhibited the best performance characteristics of the four tested. For throat heights of 104 percent T-L to 110 T-L, subsonic diffuser D showed at least 0.25 percent improvement in total-pressure recovery over diffuser A for the range of throat height tested.

~~(Secret)~~ The variation of engine-face total-pressure recovery and engine-face distortion (inboard and outboard) as functions of total engine mass-flow ratio are shown in Fig. 16 for the throat height (110 percent T-L) that provided the highest peak recovery. Diffuser D at peak recovery showed approximately a 0.5-percent increase in total-pressure recovery over diffuser A, and the difference increased at the higher mass-flow ratios. Diffuser D showed a lower distortion than A at the higher mass-flow ratios for both inboard and outboard engines.

~~(Secret)~~ Subsonic diffuser D was selected as the primary subsonic diffuser for further studies; it showed the best average engine-face total-pressure recovery and in general showed less difference in distortion between the inboard and outboard stations than the other configurations.

### 4.4 PERFORMANCE IMPROVEMENT

~~(Secret)~~ Diffuser D was selected (Section 4.3) for continued testing to improve the inlet performance characteristics. Various porosity patterns for boundary-layer control (Fig. 3a) and vortex generators added to the interior surfaces of the duct at various locations on the ramp and cowl (Fig. 17) were tested. A list of the various items of model geometry comprising each configuration is included in Table I.

**DECLASSIFIED / UNCLASSIFIED**~~SECRET~~

## DECLASSIFIED / UNCLASSIFIED

~~(Secret)~~ The effect of vortex generator location in the duct on inlet performance is shown in Fig. 18. Maximum average engine-face total-pressure recovery is approximately equal for the three locations tested. The greatest margin in mass-flow ratio (from the condition of maximum recovery to the engine requirement) occurs for the middle and forward positions, with the forward position exhibiting slightly less engine-face distortion.

~~(Secret)~~ Variation of the average engine-face total-pressure recovery as a function of throat height is shown in Fig. 19 for configurations 7, 14, and 19, for  $M_\infty = 2.20$ ,  $\alpha = 4.0$  deg, and  $\psi = 0$  deg. The maximum total-pressure recovery for these configurations occurred for a band of throat heights from 102 to 110 percent of the unstart throat height. Comparison of the results for configurations 7 and 14 shows that porous bleed improved recovery. Little or no additional recovery was obtained through the addition of forward vortex generators (configuration 19).

~~(Secret)~~ The variations of average engine-face total-pressure recovery and of engine-face total-pressure distortion as a function of the total engine mass-flow ratio for configurations 7, 14, and 19 are shown in Fig. 20. The improvement in the maximum pressure recovery (approximately 0.8 percent) of configuration 14 over that of configuration 7 is apparently due to the effect of the change in the boundary-layer control bleed pattern (percent porosity) between J8 and J4. A comparison of the bleed arrangement and percent porosity of the two configurations can be seen in Fig. 3.

~~(Secret)~~ The vortex generators installed in the forward position (configuration 19) caused a one-percent decrease in engine-face average total-pressure recovery along the engine operating line compared to configuration 14 with no vortex generators. As a result of the addition of the vortex generators, the engines experienced an apparent one-percent decrease in distortion at the inboard engine and a two-percent decrease at the outboard engine.

#### 4.5 EFFECT OF MACH NUMBER ON INLET PERFORMANCE

~~(Secret)~~ Configurations 22 and 27, with subsonic diffuser D, bleed pattern J8, and vortex generator V5, were selected for a Mach-number performance evaluation. Inlet performance characteristics are presented in the form of compressor-face total-pressure recovery and total-pressure distortion for each simulated engine compressor face as a function of single engine mass-flow ratio. The performance data at

~~SECRET~~  
DECLASSIFIED / UNCLASSIFIED

transonic Mach numbers are presented for a throat height of 3.11 in.; at the higher Mach numbers (2.00 and 2.20), the data are presented for a throat height of 110 percent T-L.

(~~Secret~~) The effect of Mach number on the air-induction system performance measured at each of the simulated engine compressor faces is presented in Fig. 21. The total-pressure distortion for the inboard engine is generally higher than that for the outboard engine, particularly at the higher mass-flow ratios. Also, the inboard engine generally had a lower total-pressure recovery than the outboard engine in the transonic Mach range. This was expected because less flow turning was required for the outboard engine than for the inboard engine. The inboard engine-simulator metering duct apparently did not have sufficient pressure ratio to obtain the desired airflows at  $M_\infty = 0.6$ , as shown in Fig. 21a.

(~~Secret~~) It was observed that the mass-flow ratio at which inlet instability (buzz) occurred increased with increasing Mach number.

#### 4.6 EFFECT OF ANGLE OF ATTACK ON INLET PERFORMANCE

(~~Secret~~) To define the effect of model angle of attack on inlet performance, data were recorded at various angles of attack from 0.2 to 13.0 deg.

(Unclassified) Because the angle-of-attack effect was not consistent over the Mach number range tested, the inlet performance is discussed according to operation at low, medium, and high Mach numbers. Inlet performance characteristics are presented in Fig. 22 to show the effect of model angle of attack on engine-compressor-face total-pressure recovery and total-pressure distortion as a function of the total engine mass-flow ratio.

##### 4.6.1 Mach Number = 0.60 and 0.95 (Low Range)

(~~Secret~~) In Fig. 22a the effect of angle of attack on inlet performance is negligible from  $\alpha = 0.2$  to 4.0 deg for the Mach number of 0.60, at mass-flow ratios less than 0.80. At  $\alpha = 13$  deg an additional two-percent loss in recovery occurred at the high mass-flow ratios. As the mass-flow ratio was increased above 0.80, there was a rapid decrease in total-pressure recovery and an increase in distortion.

(~~Secret~~) The most notable evidence of the effect of angle of attack on distortion was that the inboard engine exhibited consistently

~~SECRET~~  
DECLASSIFIED / UNCLASSIFIED

~~SECRET~~

AEDC-TR-67-213

DECLASSIFIED / UNCLASSIFIED

higher distortion than the outboard engine over the entire range of mass-flow ratios.

(~~Secret~~) The effect of model angle of attack on inlet performance at the Mach number of 0.95 is shown in Fig. 22b. These data also show that the distortion for the inboard engine was greater than that for the outboard engine, but the difference does not appear to be as great, in the range of mass-flow ratios corresponding to the engine requirement, as was found for the performance at a Mach number of 0.60.

#### 4.6.2 Mach Number = 1.50 (Medium Range)

(~~Secret~~) Figure 22c shows a definite increase in engine-face total-pressure recovery as the angle of attack was increased from 0.2 to 13.0 deg over a wide range of mass-flow ratios. At a mass-flow ratio 0.76, corresponding to the engine requirement (Ref. 3), the gain in total-pressure recovery, as angle of attack was increased from 0.2 to 13.0 deg, was approximately 1.0 percent.

(~~Secret~~) The effect of angle of attack on the pressure distortion at a mass-flow ratio about 0.76 did not appear to be direct function of angle of attack. The tendency for the inboard engine to consistently exhibit higher values of distortion than the outboard engine (as noted previously in the low Mach number range) was not evident, except at conditions of  $\alpha = 8.0$  deg.

#### 4.6.3 Mach Number = 2.00 and 2.20 (High Range)

(~~Secret~~) Maximum engine-face total-pressure recoveries of 0.930 and 0.925 were obtained at  $\alpha = 4.0$  deg at Mach numbers 2.00 and 2.20 (Figs. 22d and e, respectively). At airflows corresponding to the referenced engine requirements, the recoveries were about one and two percent lower at the respective Mach numbers and the distortions were essentially equal at 0.045 for the inboard engine.

(~~Secret~~) Distortion was generally greater for the inboard engine than for the outboard engine for  $\alpha = 0.2$  and 4.0 deg for both Mach numbers at mass-flow ratios up to about 0.85. At the high angles of attack of 8.0 and 11.0 deg, this relationship was reversed.

### 4.7 EFFECT OF YAW ANGLE ON INLET PERFORMANCE

(~~Secret~~) The configuration selected for the performance evaluation [diffuser I2 (D), boundary-layer bleed J8, and VG pattern V5]

~~SECRET~~

DECLASSIFIED / UNCLASSIFIED

~~SECRET~~  
DECLASSIFIED / UNCLASSIFIED

was tested at various yaw angles from  $-5.0$  to  $5.0$  deg. Inlet performance characteristics are presented in Fig. 23 to show the effect of yaw angle on engine-compressor-face total-pressure recovery and distortion as a function of total engine mass-flow ratio at  $4.0$ -deg angle of attack.

(~~Secret~~) The data at the low Mach numbers ( $0.60$  and  $0.95$ ), Figs. 23a and b, show that the effect of positive yaw on inlet performance was negligible. However, yawing the model  $-5.0$  deg produced a total-pressure recovery loss up to two percent, and the engine-face pressure distortion increased a corresponding amount at Mach number  $0.60$ . Little effect of yaw on total-pressure distortion was indicated at Mach number  $0.95$ .

(~~Secret~~) The data for the medium Mach number ( $1.50$ ), Fig. 23c, show that the engine-face total-pressure recovery increased slightly as yaw angle was increased from zero to  $5.0$  deg. A decrease in engine-face total-pressure recovery up to three percent is shown for the negative yaw angles. The minimum engine-face total-pressure distortion occurred at  $2.5$ -deg yaw and the maximum occurred at  $-5.0$  deg.

(~~Secret~~) Inlet performance was directly affected by yaw angle at the high Mach numbers ( $2.00$  and  $2.20$ ) as shown in Figs. 23d and e. Generally, an increase in average inlet total-pressure recovery and mass-flow ratio was shown as yaw angle was increased from  $-5.0$  to  $5.0$  deg. Engine-face total-pressure distortion showed little effect from yaw angle from zero to  $5.0$  deg; however, at negative yaw angles the distortion doubled.

(~~Secret~~) At a Mach number of  $2.00$  the use of a bypass system would be required at all yaw angles except zero and  $-2.5$  deg to match the engine reference airflows.

(~~Secret~~) At a Mach number of  $2.20$  (Fig. 23e) engine-face total-pressure recovery showed a direct increase with increasing angle of yaw from  $-2.5$  to  $5.0$  deg. The maximum recovery and minimum distortion were obtained at  $5.0$ -deg yaw. Yawing the model  $5.0$  deg increased engine-face pressure recovery four percent at the engine reference airflow. The effect of yaw angle on total-pressure distortion was small except for  $-5.0$  deg, where the fuselage tended to block the flow to the inlet and thus resulted in an increase in distortion and reduced recovery. This blockage of flow from the inlet at  $-5.0$  deg yaw was seen in the boundary-layer data discussed in Section 4.1 (Fig. 11).

DECLASSIFIED / ~~SECRET~~  
DECLASSIFIED / UNCLASSIFIED

## DECLASSIFIED / UNCLASSIFIED

(~~Secret~~) For all Mach numbers, distortion was greater for the inboard engine than for the outboard engine at negative yaw angles or for the high supercritical conditions. Also for all Mach numbers, the loss in total-pressure recovery and increase in total-pressure distortion for negative yaw angles was greater than the gain at positive yaw angles.

### 4.8 EFFECT OF THROAT HEIGHT ON INLET PERFORMANCE

(~~Secret~~) The peak engine-face total-pressure recovery as a function of throat height in percent T-L for the selected configuration 19 is presented in Fig. 24. These data show that the total-pressure recovery between 104 percent T-L and 110 percent T-L was less sensitive to throat height. Above or below these values the total-pressure recovery made a significant drop. Figure 25 presents performance data for two throat heights at  $M_\infty = 2.20$  and two throat heights at  $M_\infty = 1.75$ . At  $M_\infty = 2.20$  for the engine match-line, the total-pressure recovery was higher and the total-pressure distortion was lower for the 110 percent T-L compared to the 104 percent T-L throat height. The lower limit for started inlet operation at each throat height occurred at the minimum mass-flow ratio for each of the performance curves shown. As throat height was increased the minimum mass-flow ratio required to maintain a started inlet increased. At  $M_\infty = 1.75$  (Fig. 25b) the average total-pressure recovery was relatively insensitive to the throat-height settings investigated. However, below a mass-flow ratio of 0.825 the small throat height gave the lowest distortion for both inboard and outboard engines. Therefore, distortion would be the factor in determining the throat height at  $M_\infty = 1.75$ . For the Mach numbers below 1.75 a throat height of 3.11 in. was maintained. At this throat height the first and second ramps were aligned.

### 4.9 EFFECT OF BYPASS ON PERFORMANCE

(~~Secret~~) The NAA AMSA vehicle will use the variable bypass system to minimize spillage drag around the cowl lip, to optimize inlet engine airflow matching, and to position the internal terminal shock for optimum inlet performance. Sketches of the three bypass configurations tested are shown in Fig. 4. Bypass configuration U1 had a controlled exit door on the top diffuser wall and configurations U2 and U3 had porous diffuser walls.

(~~Secret~~) Performance data for three bypass configurations are presented in Fig. 26 to show the effect of increasing bypass flow.

~~SECRET~~  
DECLASSIFIED / UNCLASSIFIED

The inlet performance is also shown with no bypass for comparison purposes and to indicate the amount of bypass leakage with the bypass door or plug in the closed position. Opening the bypass door (Fig. 26a) had very little effect at door angles up to 15 deg. However, as the door angle was increased beyond 15 deg the effectiveness of bypass flow increased.

(~~Secret~~) Figures 26b and c show the effect of opening the bypass plug (increasing bypass flow) for the porous diffuser configurations. The performances of both configurations were quite similar. However, bypass configuration U3 had slightly higher recovery and lower distortion than either of the other two bypass configurations. The porous diffuser configurations provided more mass-flow-ratio control than those with the bypass door. The control of mass flow was essentially linear with plug position.

## SECTION V CONCLUSIONS

(~~Secret~~) The test results of a 0.10-scale AMSA inlet model tested through the Mach number range of 0.60 to 2.20 and at angles of attack and yaw from 0.2 to 13.0 deg and -5.0 to 5.0 deg, respectively, indicate that:

- (~~Secret~~) 1. Approximately a 20-percent increase in average total-pressure recovery and a larger decrease in distortion was obtained with the addition of the best boundary-layer control configuration.
- (~~Secret~~) 2. The total-pressure distortion for the inboard engine was generally higher than that of the outboard engine, particularly at the higher mass-flow ratios.
- (~~Secret~~) 3. As throat height was increased, an increase in mass-flow ratio was required to maintain a started inlet.
- (~~Secret~~) 4. Both total-pressure recovery and distortion were affected by throat height changes at  $M_\infty = 2.20$ . However, at  $M_\infty = 1.75$ , distortion was the primary factor affected by throat height.
- (~~Secret~~) 5. Bypass configuration U3 had slightly higher recovery and lower distortion than either of the other two configurations tested.

DECLASSIFIED / UNCLASSIFIED

~~SECRET~~

**DECLASSIFIED / UNCLASSIFIED**

- (~~Secret~~) 6. Both porous-bypass configurations had more bypass mass-flow-ratio control than did the bypass-door configurations.
- (~~Secret~~) 7. Buzz-free inlet operation for normal inlet geometries was obtained throughout the test range.
- (~~Secret~~) 8. The addition of vortex generators reduced distortion up to two percent, particularly for the outboard engine.

**REFERENCES**

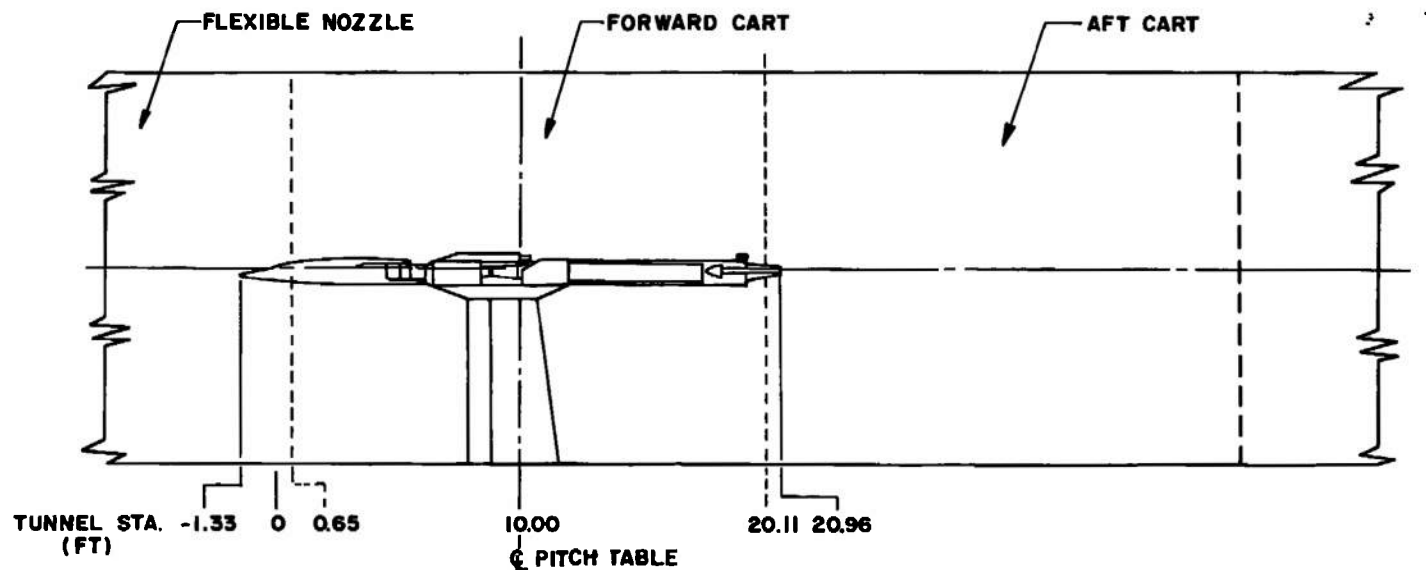
1. Test Facilities Handbook (6th Edition). "Propulsion Wind Tunnel Facility, Vol. 5." Arnold Engineering Development Center, November 1966.
2. "Test Plan Report for Series I Tests of a 0.10 Scale AMSA Inlet Model in the AEDC 16-Foot Propulsion Wind Tunnel (U)." NA-66-1354, March 2, 1967. (SECRET)
3. Boman, C. D. "Miscellaneous Task S-5 Inlet Model Data (U)." TFD 67-402, North American Aviation, Inc./Los Angeles Division, April 1967. (SECRET)

**DECLASSIFIED / UNCLASSIFIED**

**APPENDIXES**

- I. ILLUSTRATIONS**
- II. TABLE**
- III. THE INFLUENCE OF THE MODEL SUPPORT STRUCTURE  
ON THE FLOW ANGULARITY AND LOCAL MACH NUMBER  
AT TRANSONIC MACH NUMBERS**

DECLASSIFIED / UNCLASSIFIED



NOT TO SCALE

MODEL LAYOUT IN THE 16S TEST SECTION

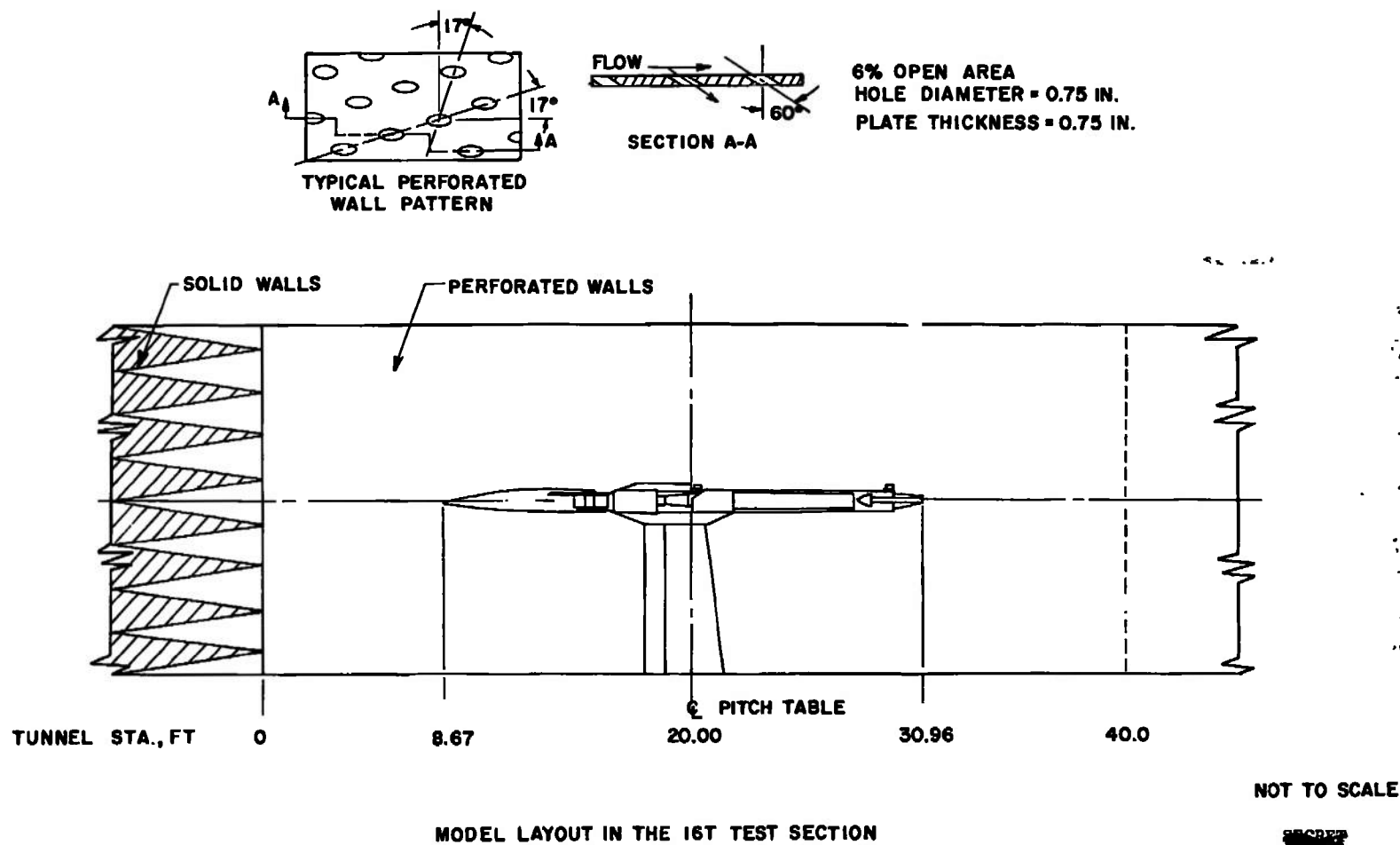
a. Tunnel 16S

Fig. 1 (Unclassified) Model Location in the Test Section

DECLASSIFIED / UNCLASSIFIED

DECLASSIFIED / UNCLASSIFIED

SECRET



b. Tunnel 16T

Fig. 1 Concluded

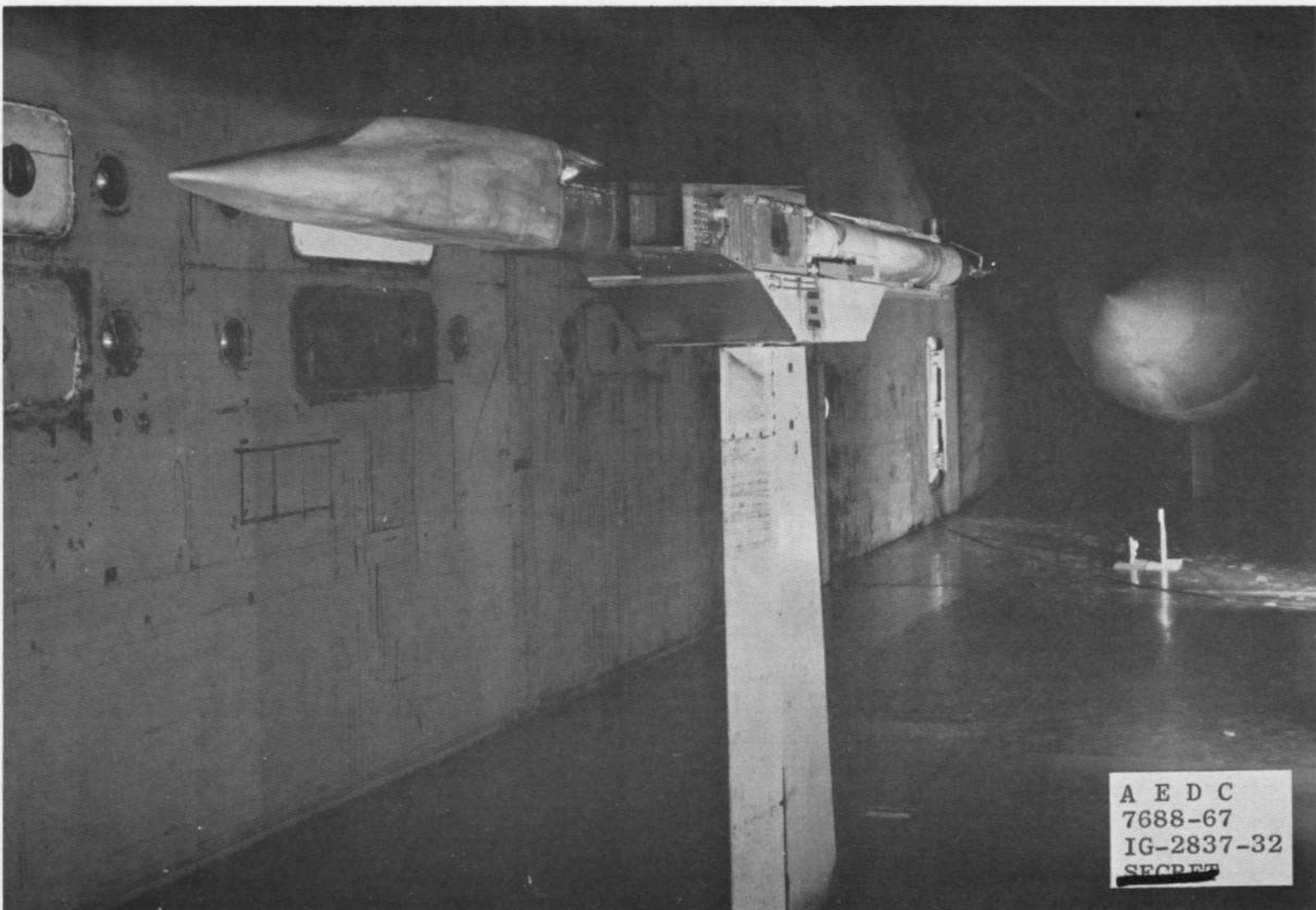
NOT TO SCALE

SECRET

~~SECRET~~

AEDC-TR-67-213

DECLASSIFIED / UNCLASSIFIED



a. Tunnel 16S

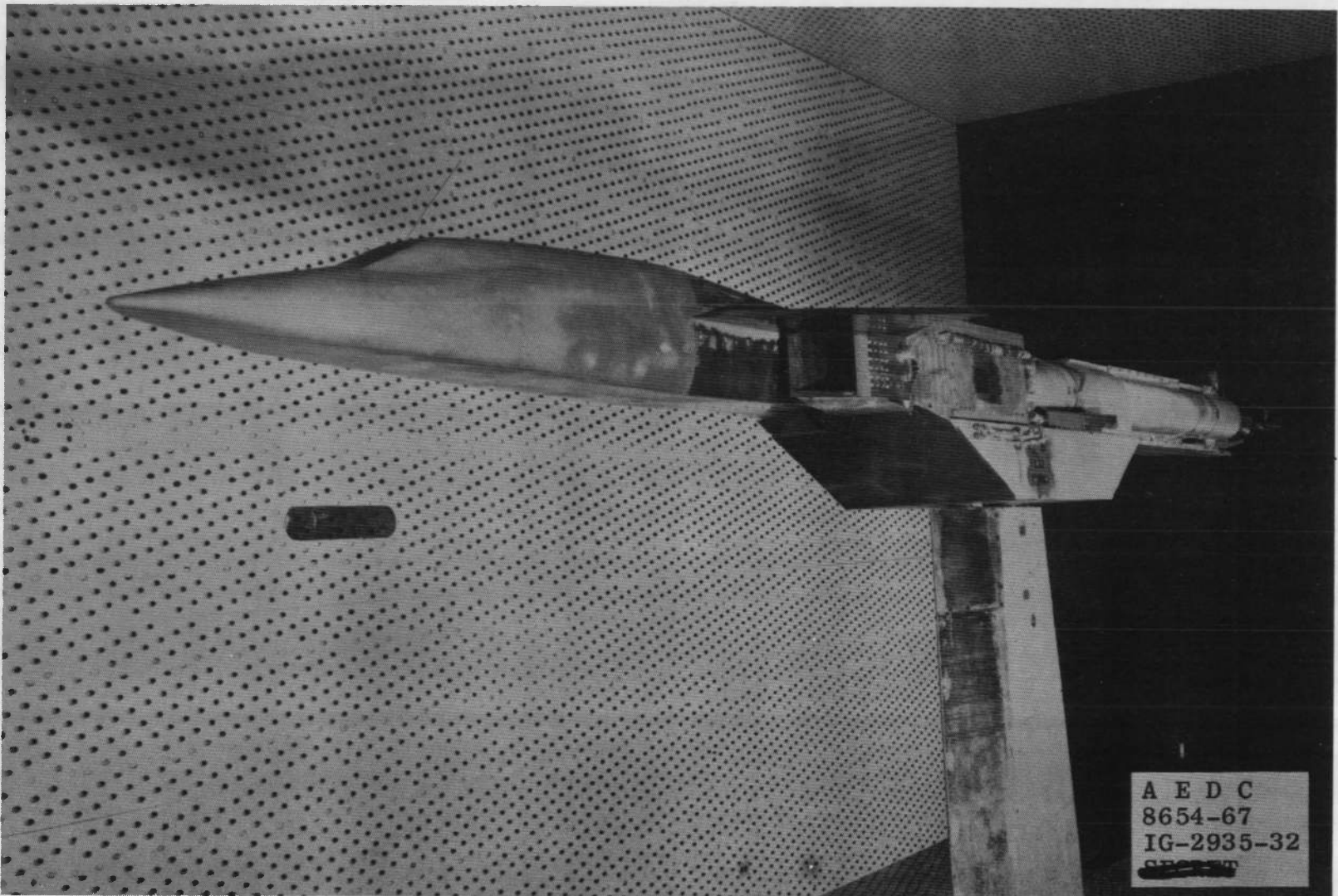
Fig. 2 (Unclassified) Model Installation

~~SECRET~~

DECLASSIFIED / UNCLASSIFIED

~~SECRET~~

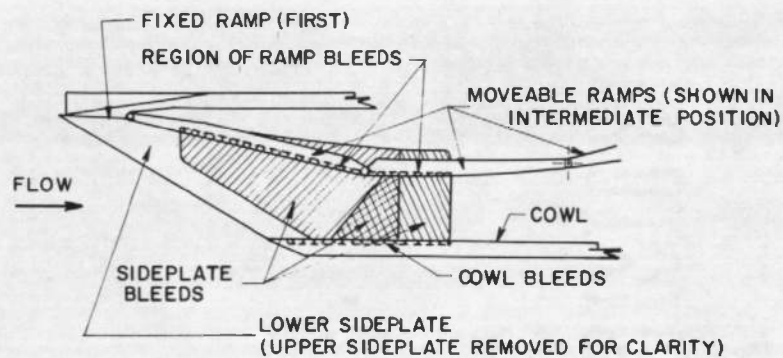
DECLASSIFIED / UNCLASSIFIED



A E D C  
8654-67  
IG-2935-32  
~~SECRET~~

b. Tunnel 16T  
Fig. 2 Concluded

DECLASSIFIED / UNCLASSIFIED

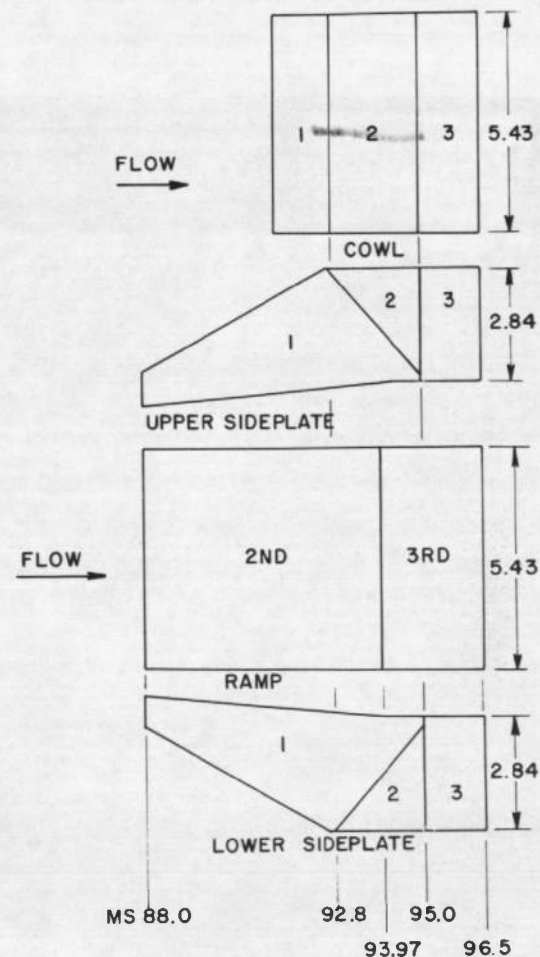


- NOTES: 1. INLET FLOW SURFACE TO BE POROUS IS DEFINED BY HEAVY SOLID LINES  
2. ALL DIMENSIONS ARE IN INCHES  
3. NOT TO SCALE

POROSITY REGIONS - POROUS MATERIAL REQUIREMENTS ~ %

CONFIG	LOWER SIDEPLATE			UPPER SIDEPLATE			COWL			RAMP	
	1	2	3	1	2	3	1	2	3	2ND	3RD
J1	11.0	11.0	11.0	11.0	11.0	11.0	3.6	4.9	7.7	7.7	11.0
J2	0.0	0.0	0.0	0.0	0.0	0.0	0.0	0.0	0.0	0.0	0.0
J3	11.0	7.7	7.7	11.0	7.7	7.7	4.9	5.7	7.7	7.7	7.7
J4	11.0	12.6	12.6	11.0	12.6	12.6	7.7	11.0	11.0	11.0	11.0
J5	11.0	7.7	7.7	11.0	7.7	7.7	3.6	4.9	7.7	11.0	7.7
J6	16.9	12.6	12.6	12.6	11.0	11.0	11.0	11.0	11.0	11.0	12.6
J7	16.9	12.6	12.6	16.9	12.6	12.6	11.0	11.0	11.0	11.0	12.6
J8	12.6	11.0	11.0	11.0	7.7	7.7	11.0	11.0	11.0	12.6	11.0
J9	12.6	11.0	11.0	11.0	7.7	7.7	11.0*	11.0	11.0	12.6	11.0

\* WITH MOVEABLE COWL, APPROXIMATELY HALF OF REGION I IS REMOVED



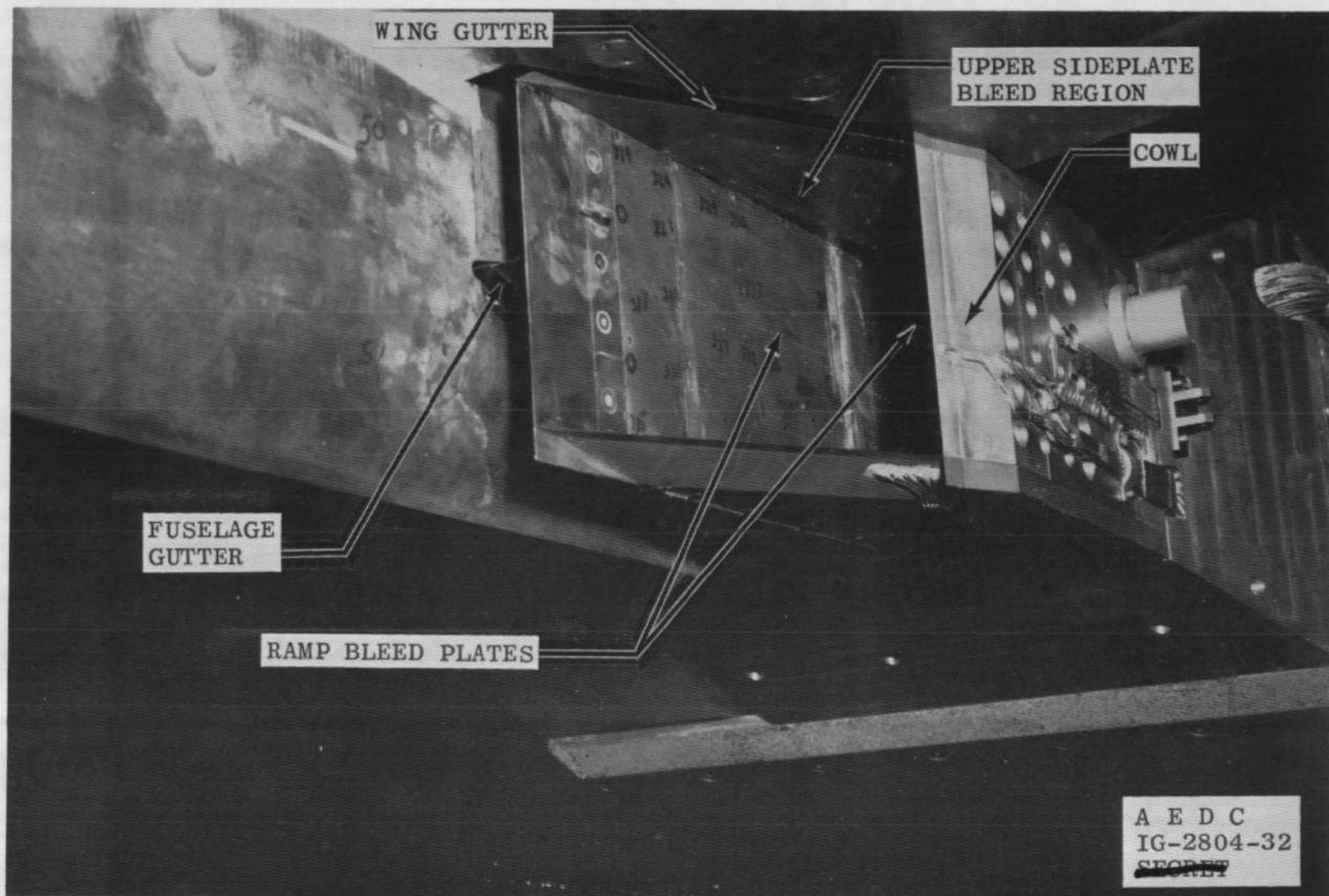
#### a. Porous Plate Locations and Percent Porosity

Fig. 3 (Unclassified) Boundary-Layer Control Configurations

~~SECRET~~

DECLASSIFIED / UNCLASSIFIED

01/22/2003



b. Boundary-Layer Gutters and Porous Plate Installation on Ramp and Upper Sideplate

Fig. 3 Concluded

DECLASSIFIED / UNCLASSIFIED

~~SECRET~~

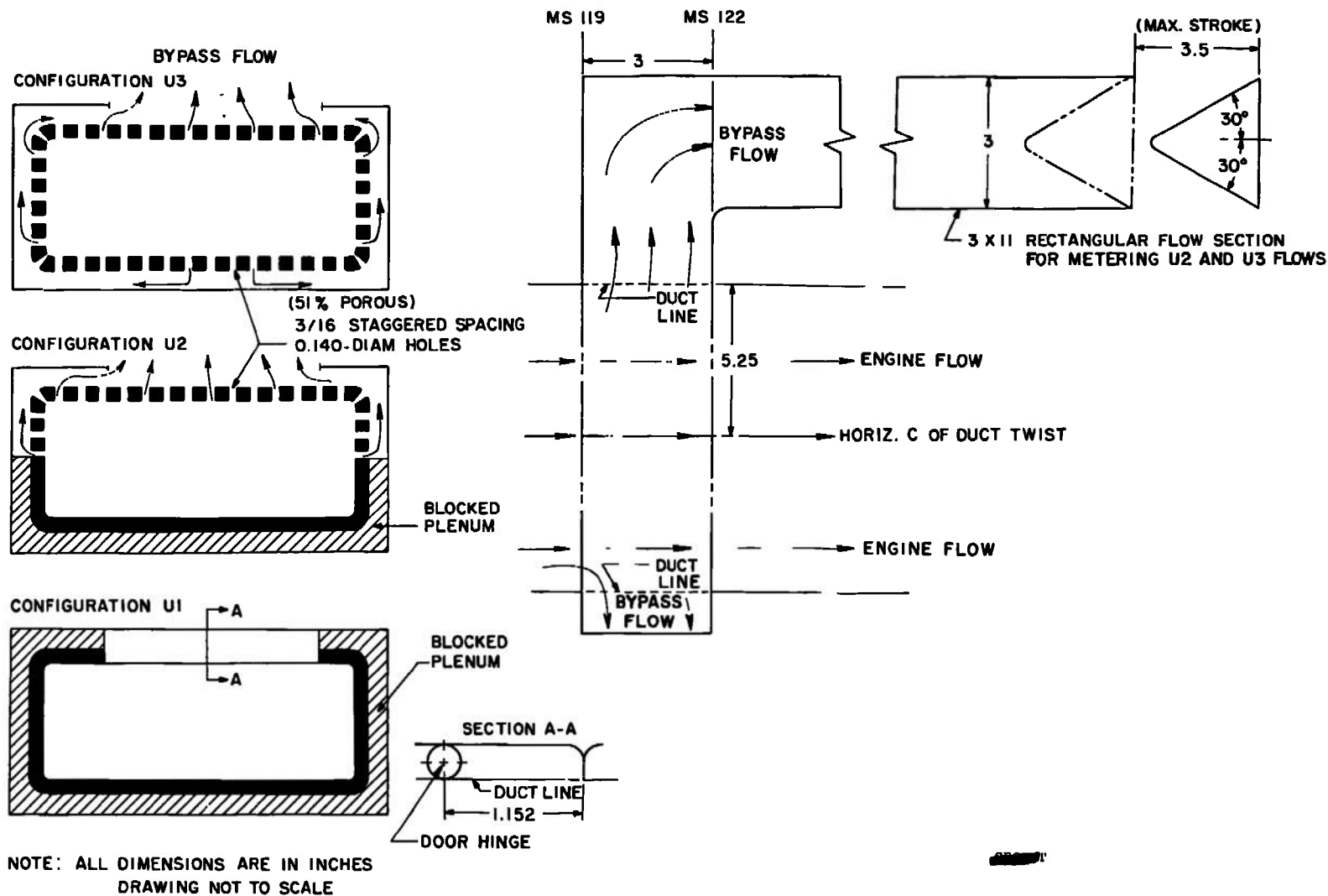
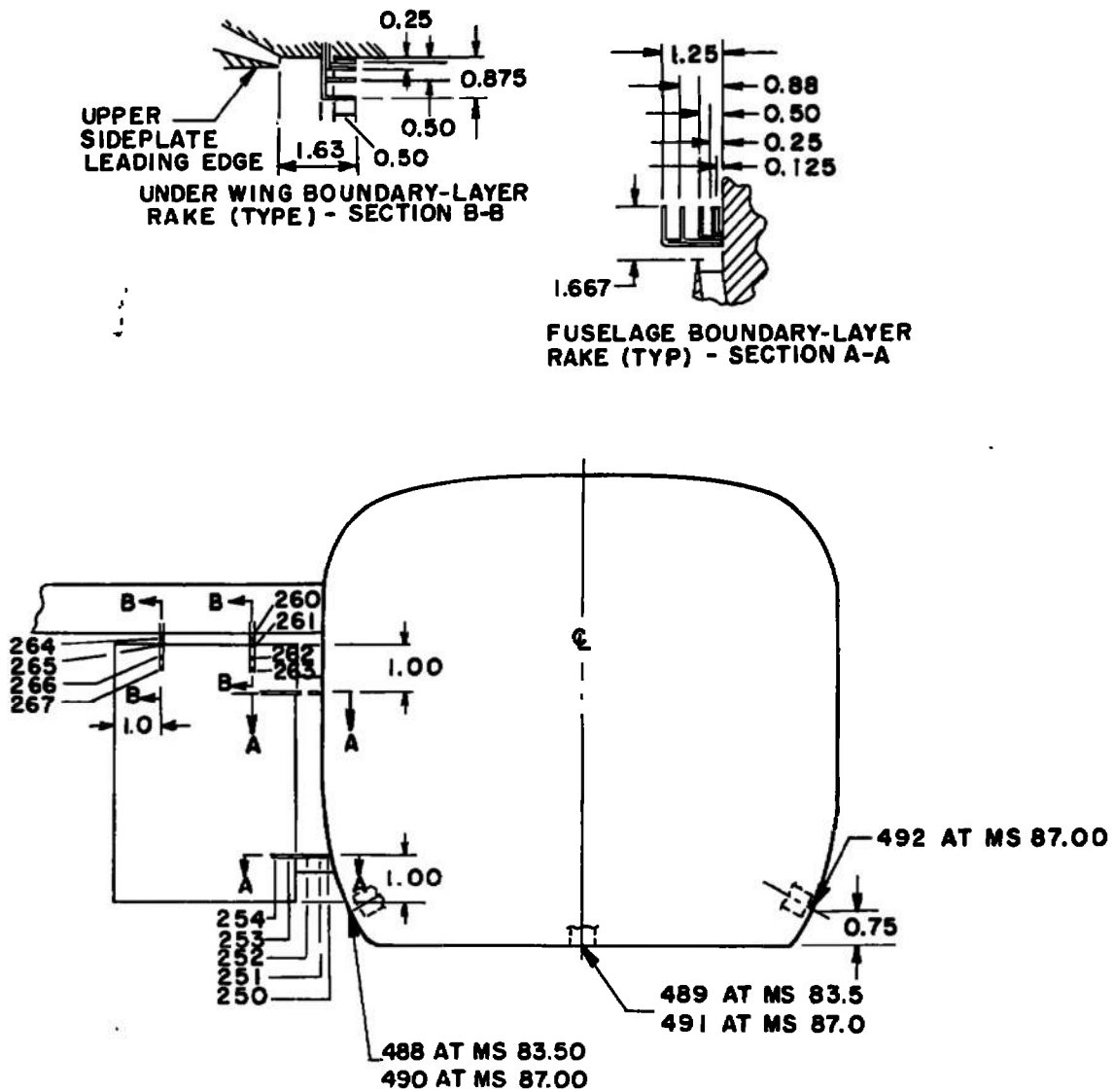


Fig. 4 (Unclassified) Bypass System Configurations

DECLASSIFIED / UNCLASSIFIED



NOTE : DIMENSIONS ARE IN INCHES

~~SECRET~~

Fig. 5 (Unclassified) Fuselage and Wing Boundary-Layer Rakes

DECLASSIFIED / UNCLASSIFIED

~~SECRET~~

DECLASSIFIED / UNCLASSIFIED

AEDC-TR-67-213

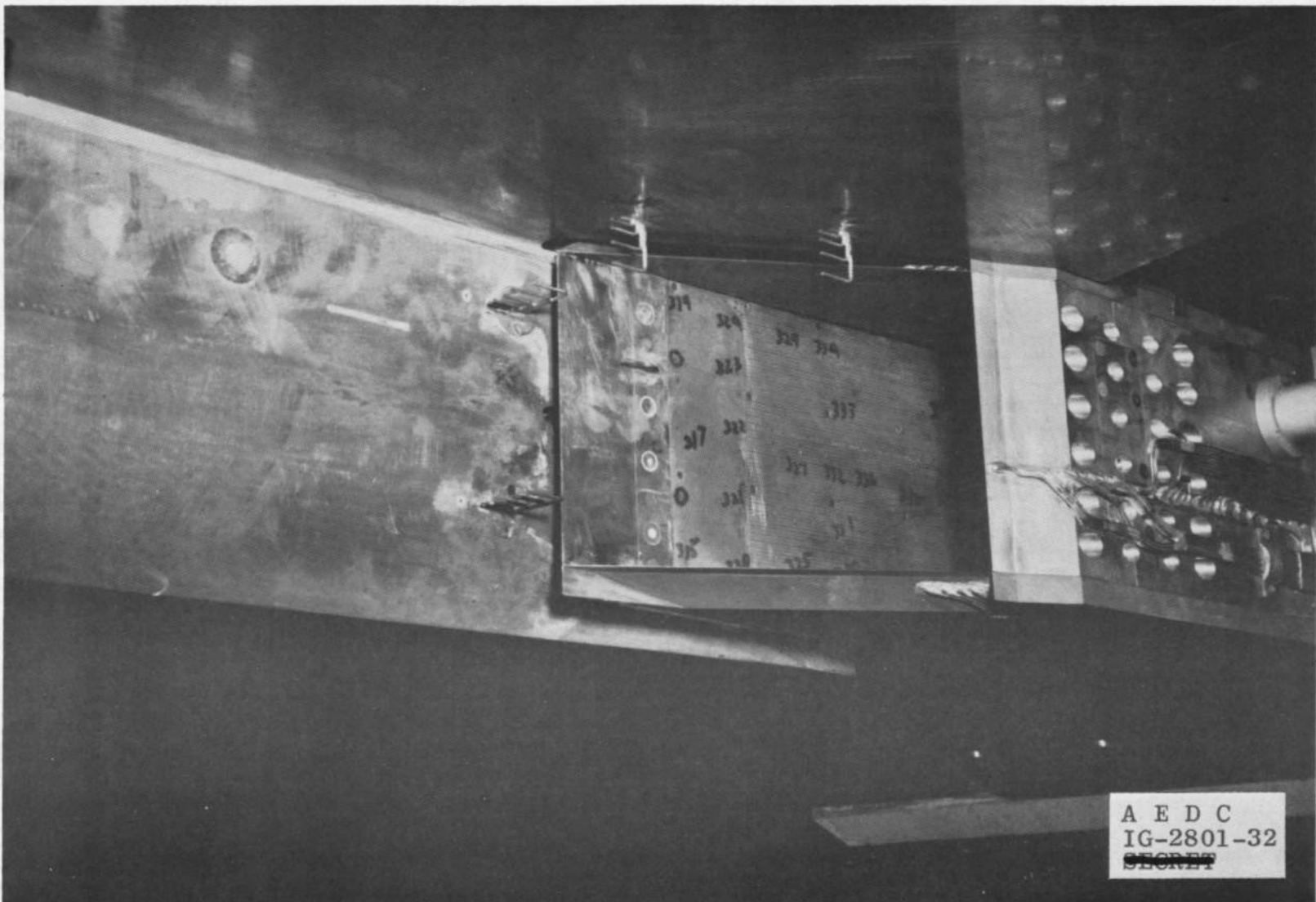


Fig. 6 (Unclassified) Photograph of Inlet Boundary-Layer Rakes

DECLASSIFIED / UNCLASSIFIED

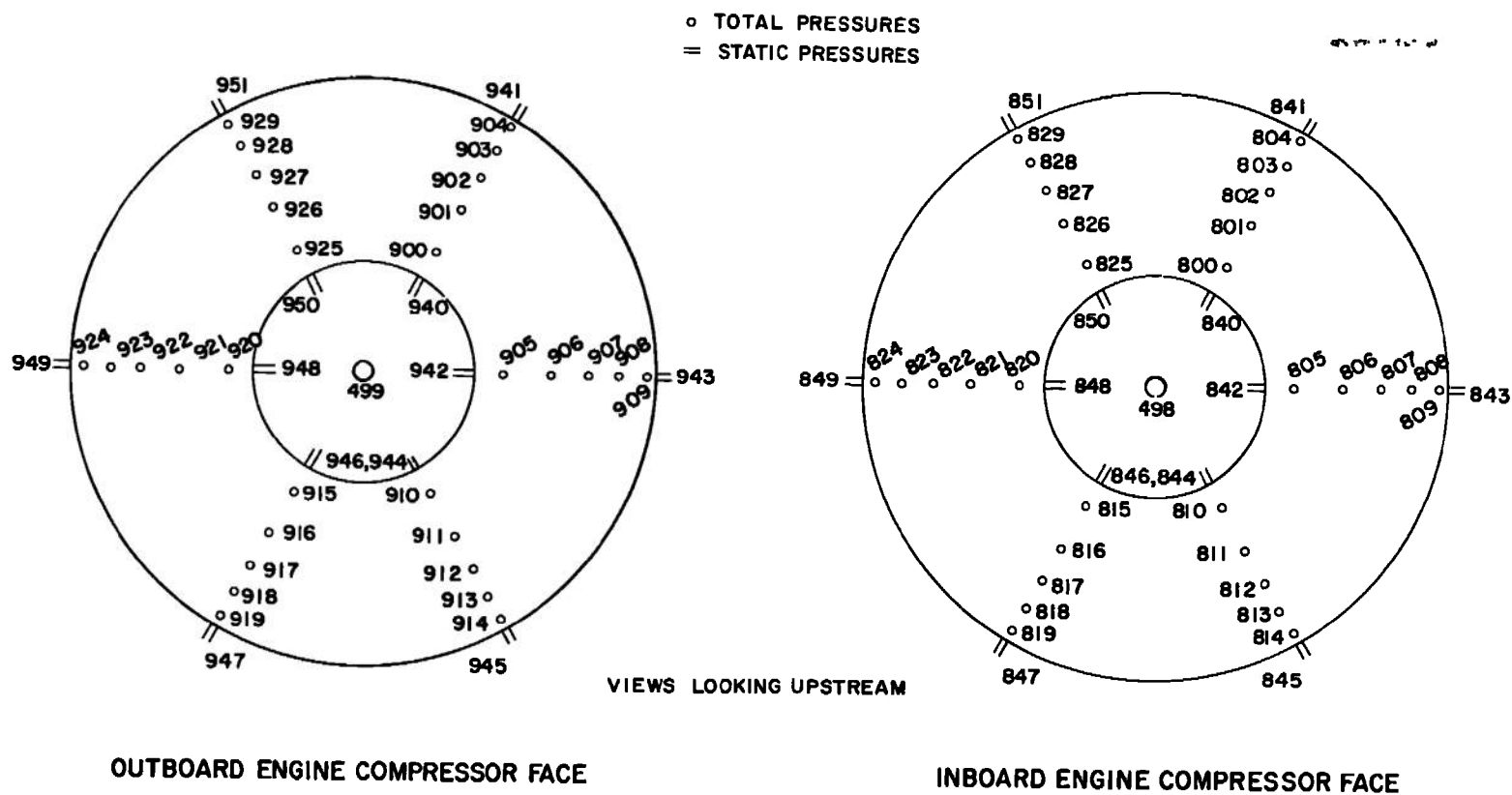


Fig. 7 (Unclassified) Compressor-Face Instrumentation

DECLASSIFIED / UNCLASSIFIED

This page is Unclassified

27

DECLASSIFIED / UNCLASSIFIED

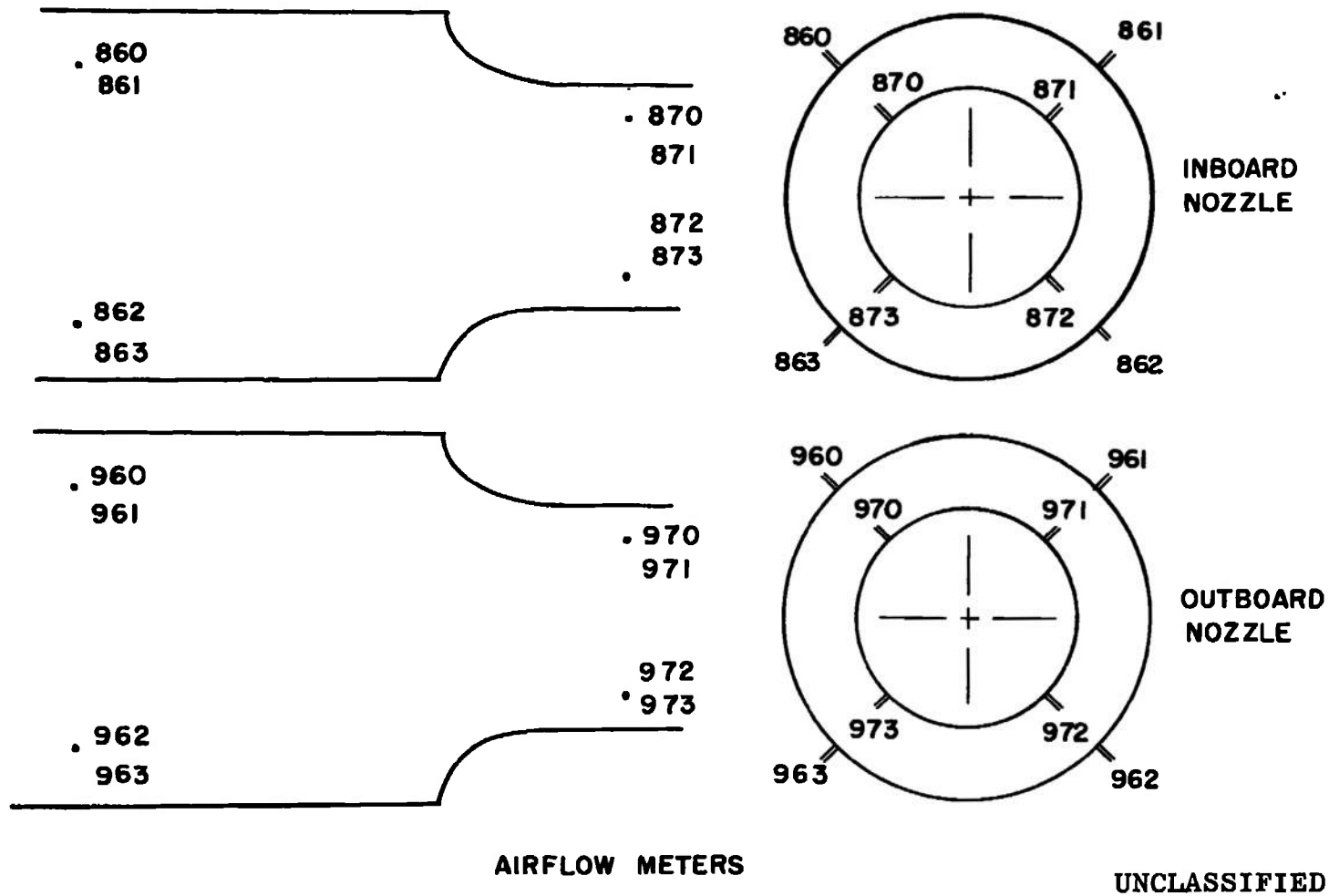


Fig. 8 (Unclassified) ASME Nozzles M1 and M2 Instrumentation

DECLASSIFIED / UNCLASSIFIED

DECLASSIFIED / UNCLASSIFIED



**Fig. 9 (Unclassified) Duct Pressure Instrumentation**

DECLASSIFIED / UNCLASSIFIED

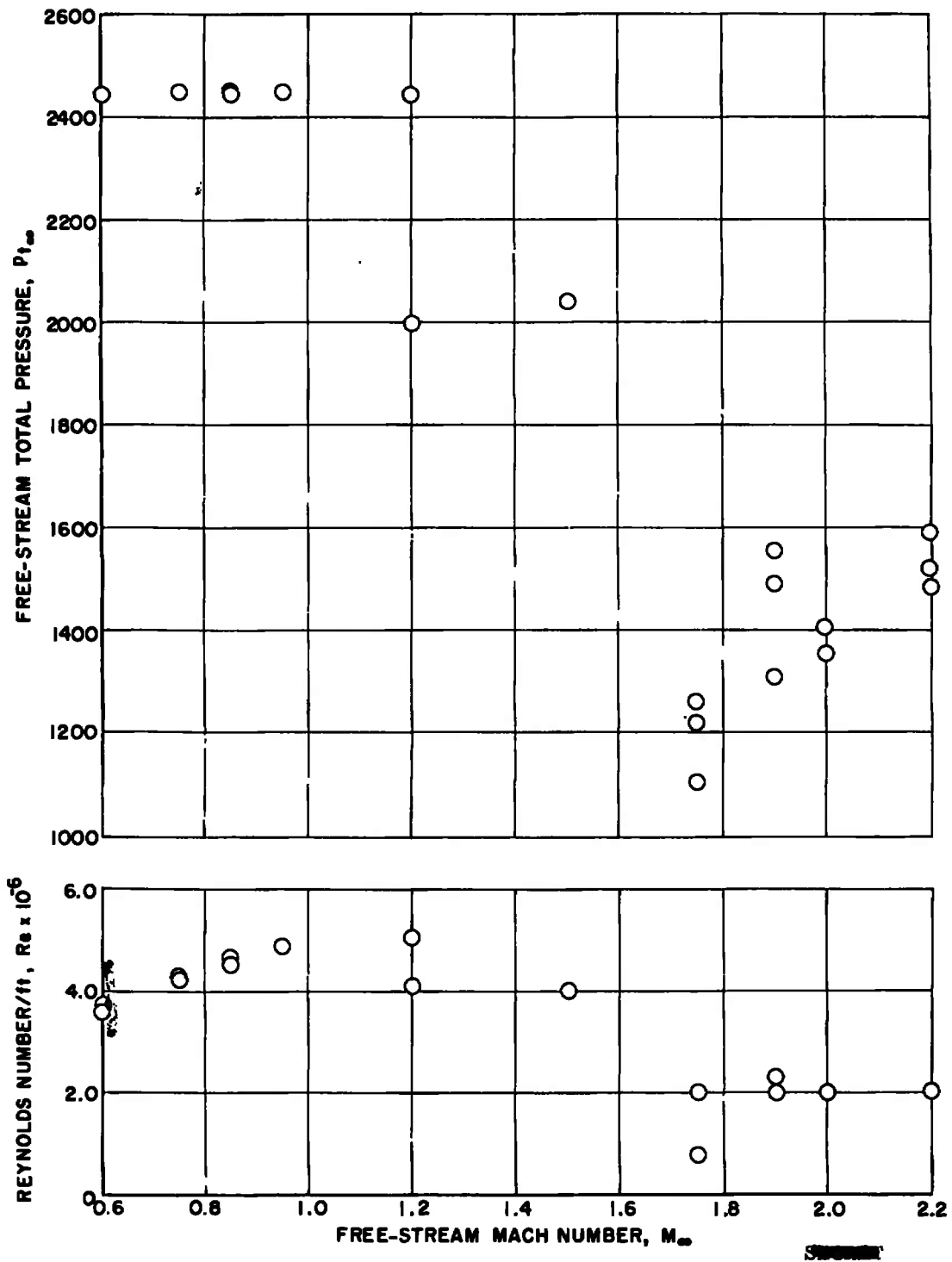
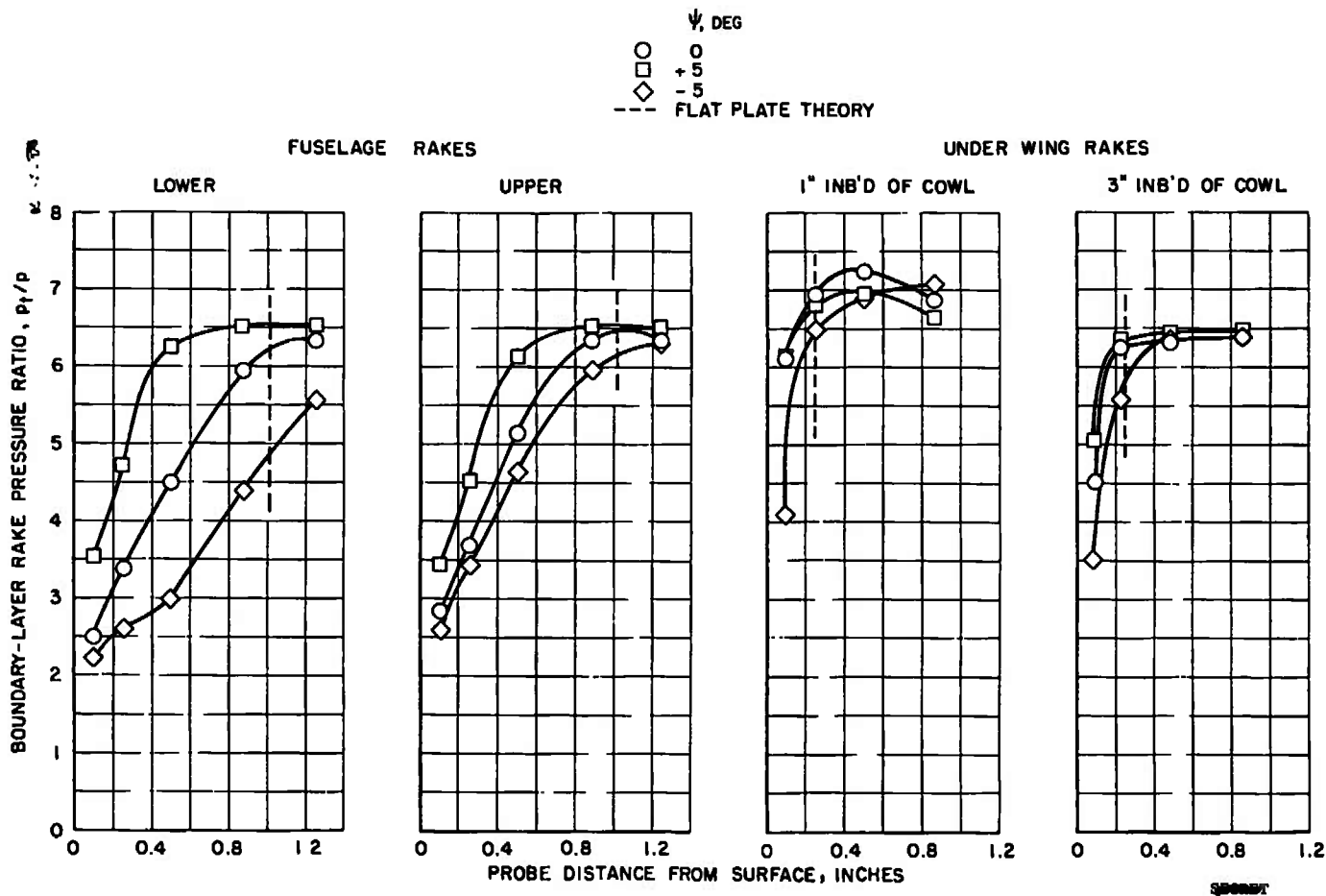


Fig. 10 (Unclassified) Summary of Test Conditions

DECLASSIFIED / UNCLASSIFIED

DECLASSIFIED / UNCLASSIFIED



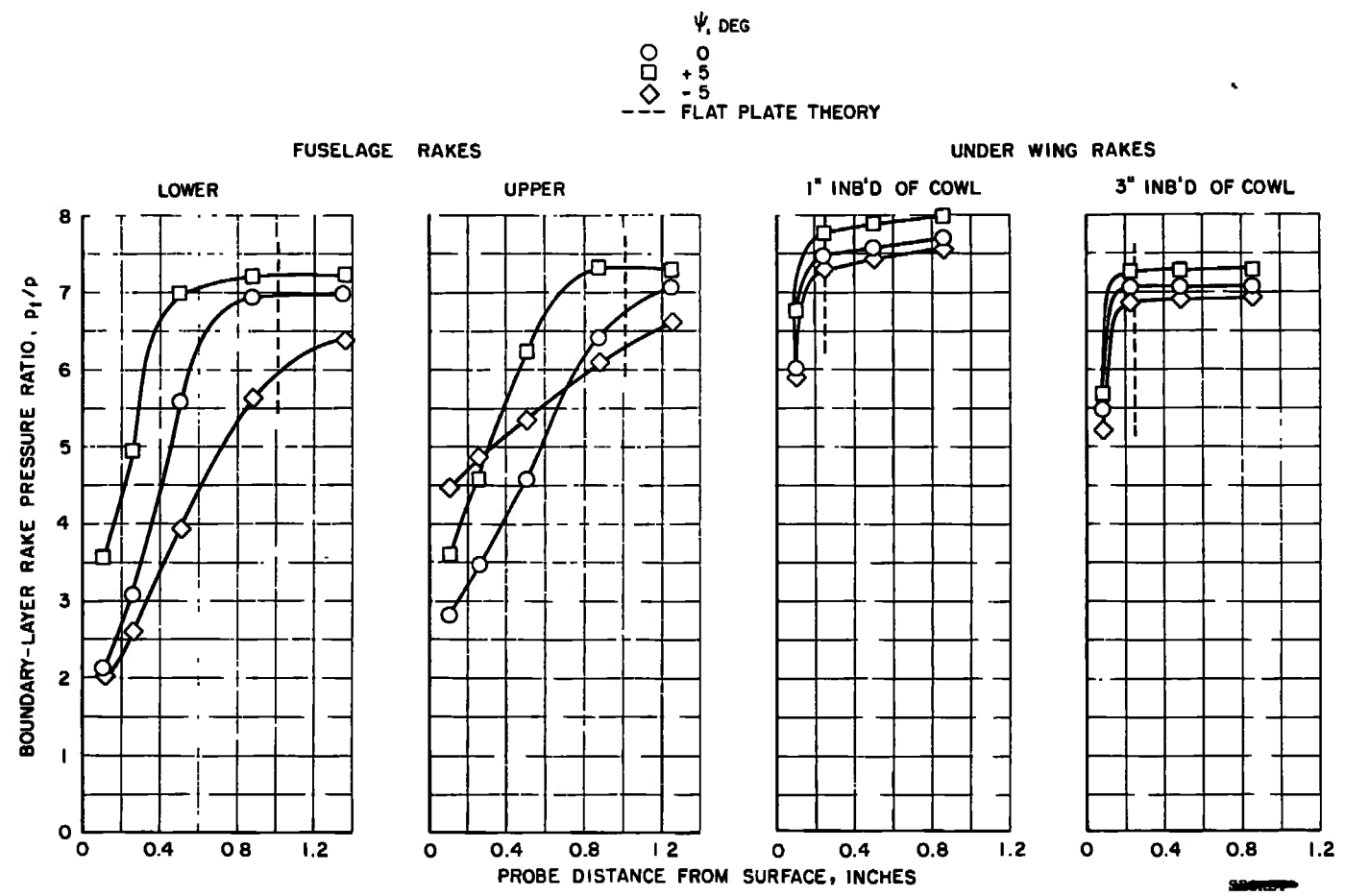
a.  $\alpha = 0.2$  deg

Fig. 11 ~~SECRET~~ Fuselage and Wing Boundary-Layer Total-Pressure Profiles at  $M_\infty = 2.20$

DECLASSIFIED / UNCLASSIFIED

31

DECLASSIFIED / UNCLASSIFIED

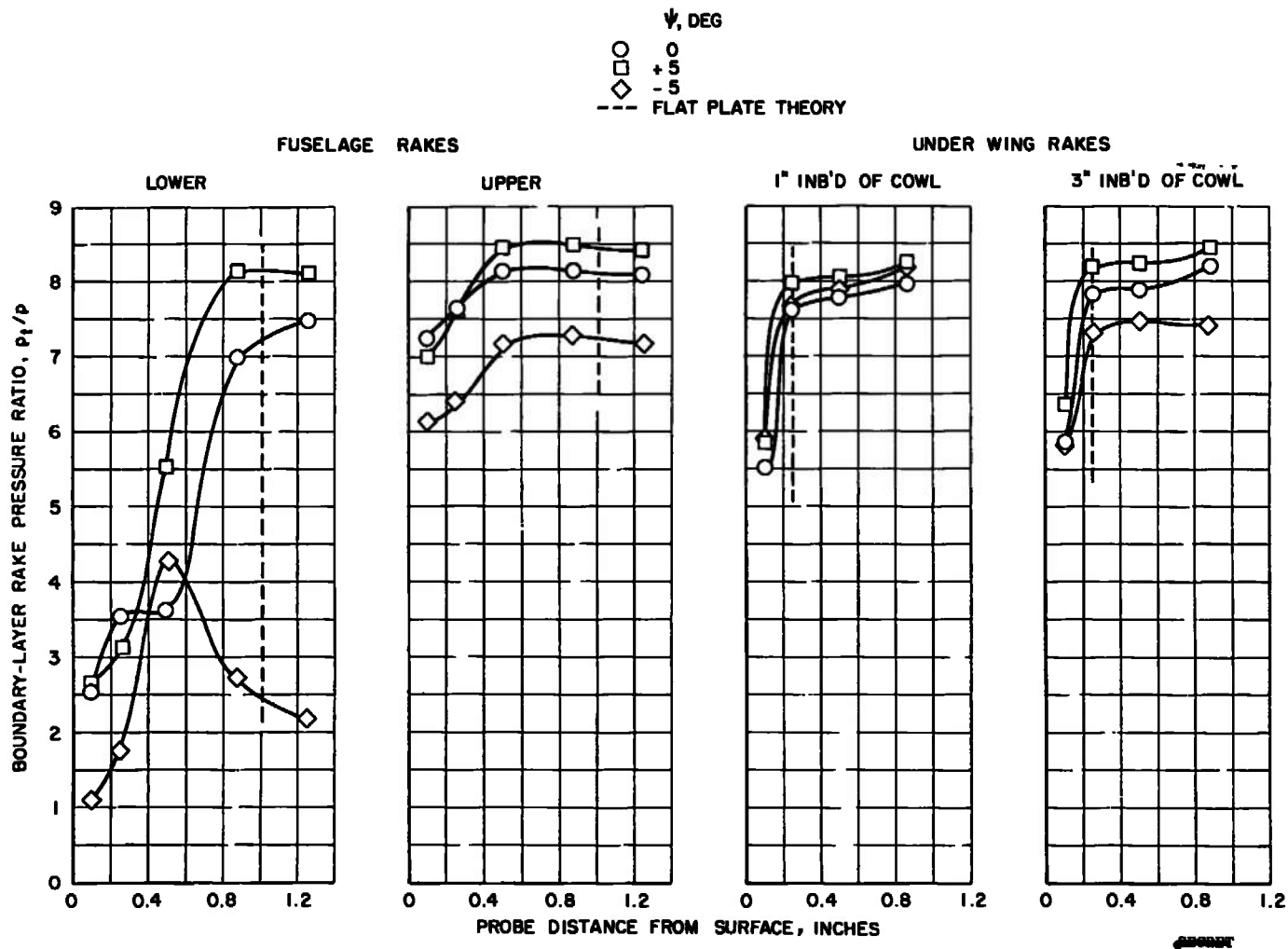


b.  $\alpha = 4.0$  deg

Fig. 11 Continued

DECLASSIFIED / UNCLASSIFIED

DECLASSIFIED / UNCLASSIFIED



c.  $\alpha = 11.0$  deg

Fig. 11 Concluded

DECLASSIFIED / UNCLASSIFIED

DECLASSIFIED / UNCLASSIFIED

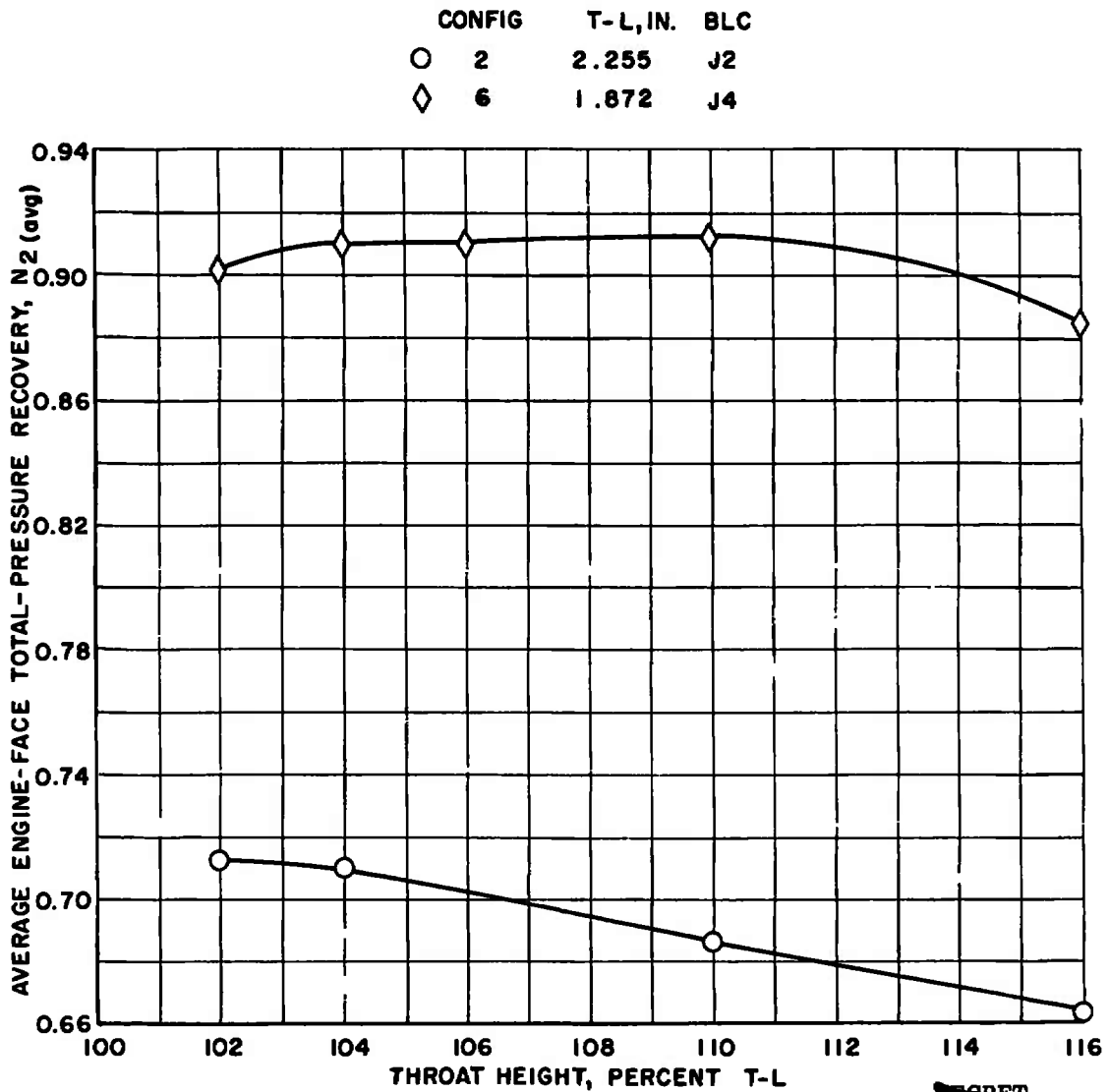


Fig. 12 ~~SECRET~~ Variation in Total-Pressure Recovery as a Function of Throat Height for BLC Configurations J2 and J4,  $M_\infty = 2.20$ ,  $\alpha = 4.0$  deg,  $\psi = 0$  deg

DECLASSIFIED / UNCLASSIFIED

DECLASSIFIED / UNCLASSIFIED

CONFIG	TH, IN.	% T-L
○ 2	2.300	102
◇ 6	2.053	110
--- ENGINE REQUIREMENT		

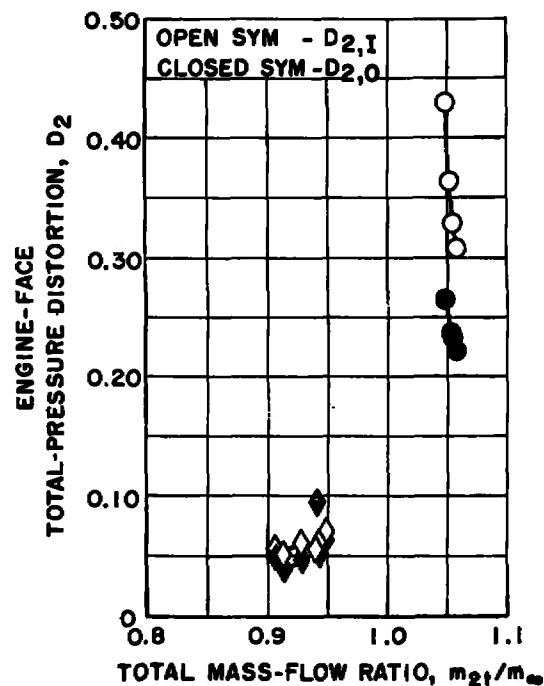
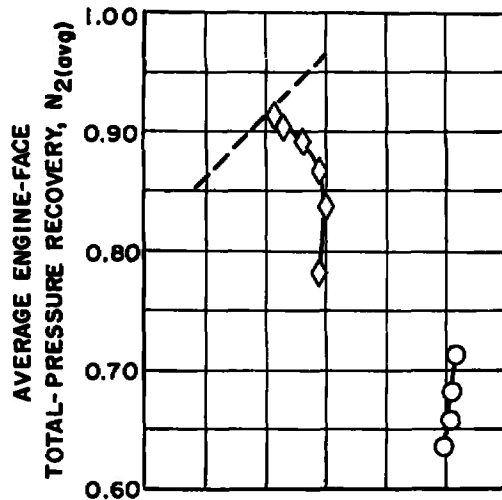


Fig. 13 (Continued) Inlet Performance BLC Configurations J2 and J4 as a Function of Mass-Flow Ratio,  $M_\infty = 2.20$ ,  $\alpha = 4.0$  deg,  $\psi = 0$  deg

DECLASSIFIED / UNCLASSIFIED

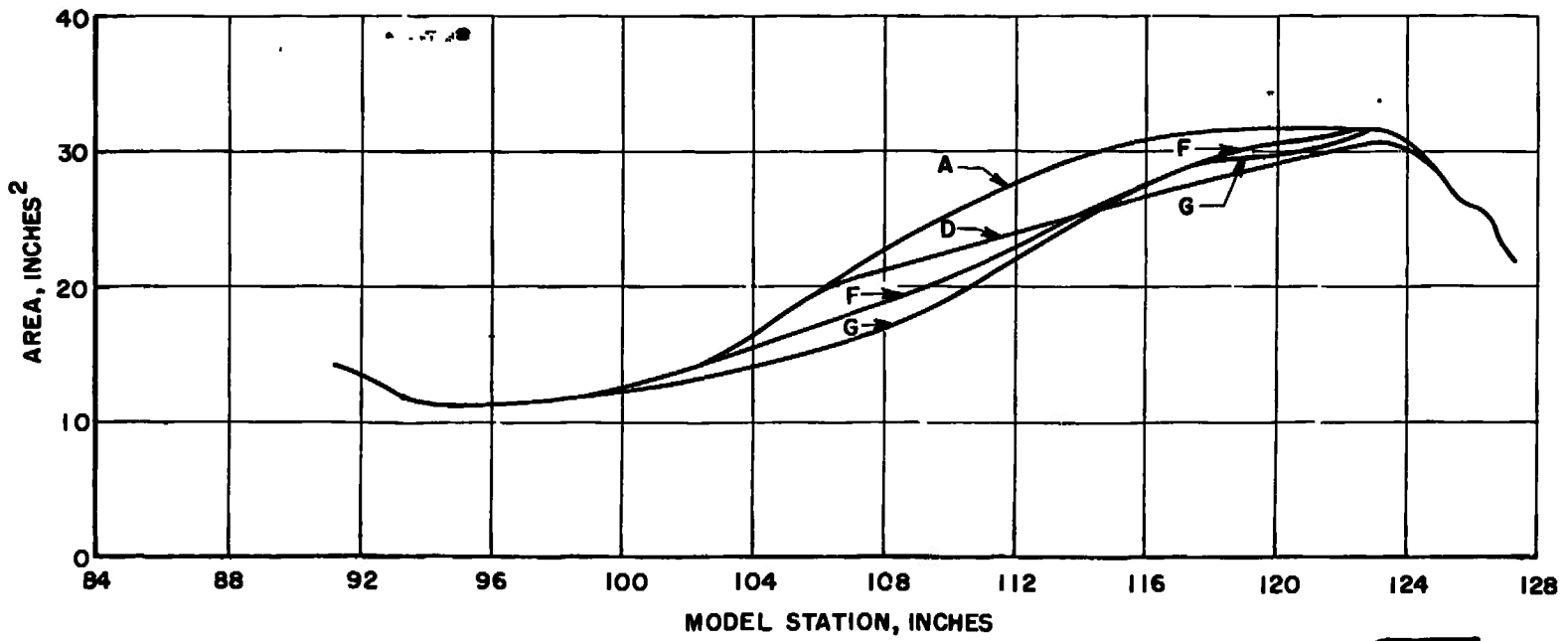


Fig. 14 (Unclassified) Subsonic Diffuser Area Distribution

DECLASSIFIED / UNCLASSIFIED

SECRET

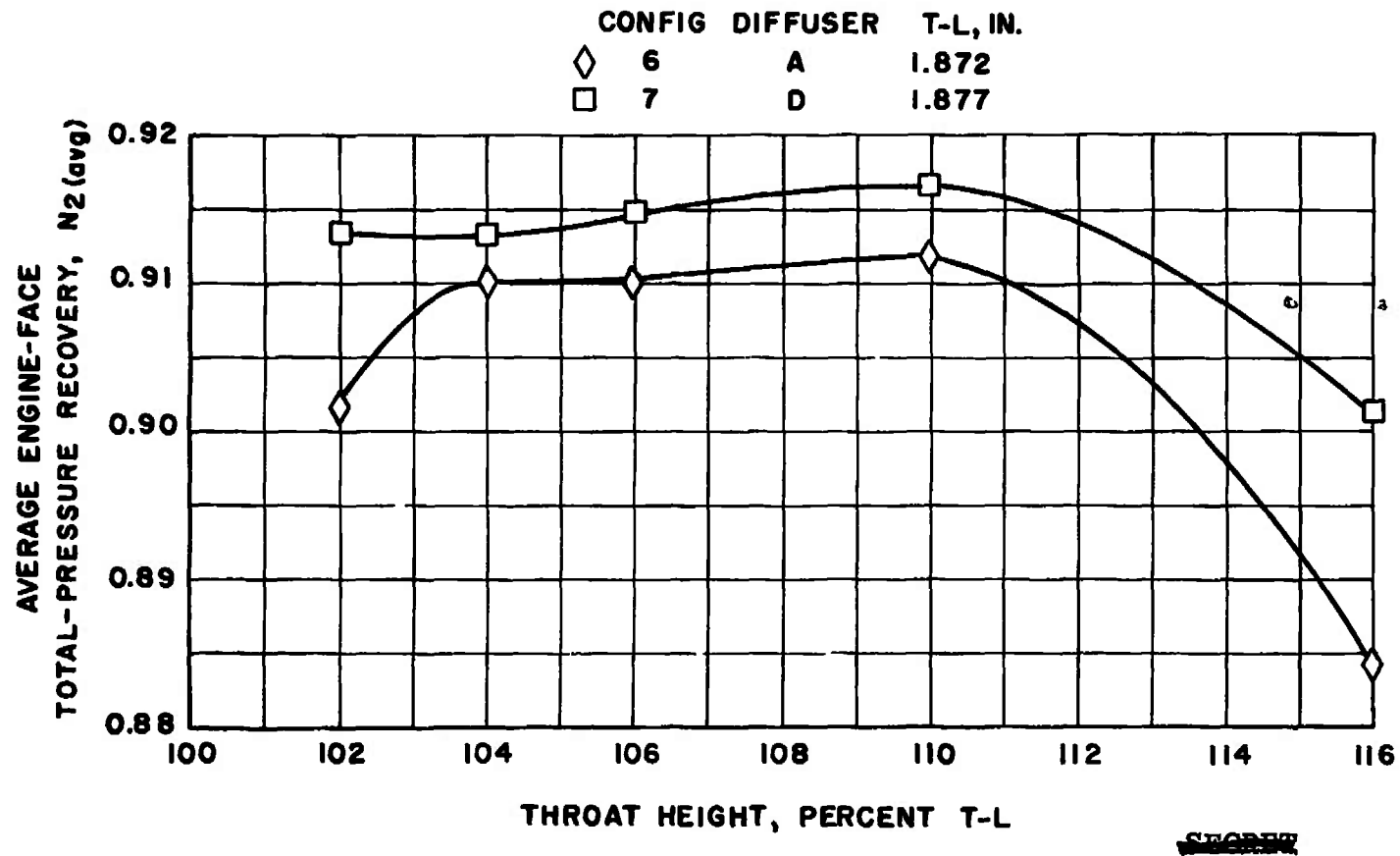


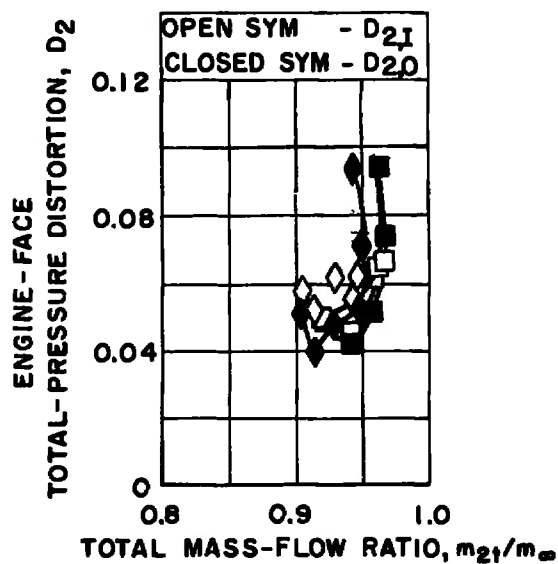
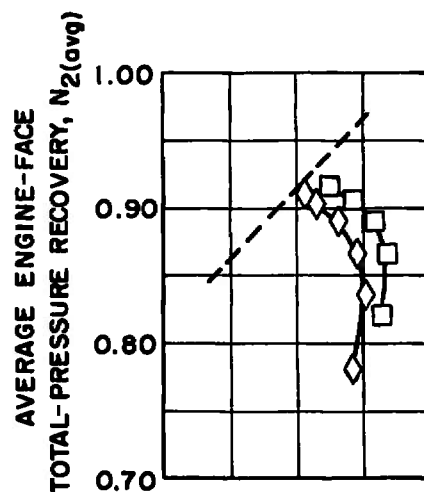
Fig. 15 (SECRET) Variation in Total-Pressure Recovery as a Function of Throat Height for Subsonic Diffusers A and D,  $M_{\infty} = 2.20$ ,  $\alpha = 4.0$  deg,  $\psi = 0$  deg

DECLASSIFIED / UNCLASSIFIED

SECRET

CONFIG	DIFFUSER	TH, IN.
◇ 6	A	2.053
□ 7	D	

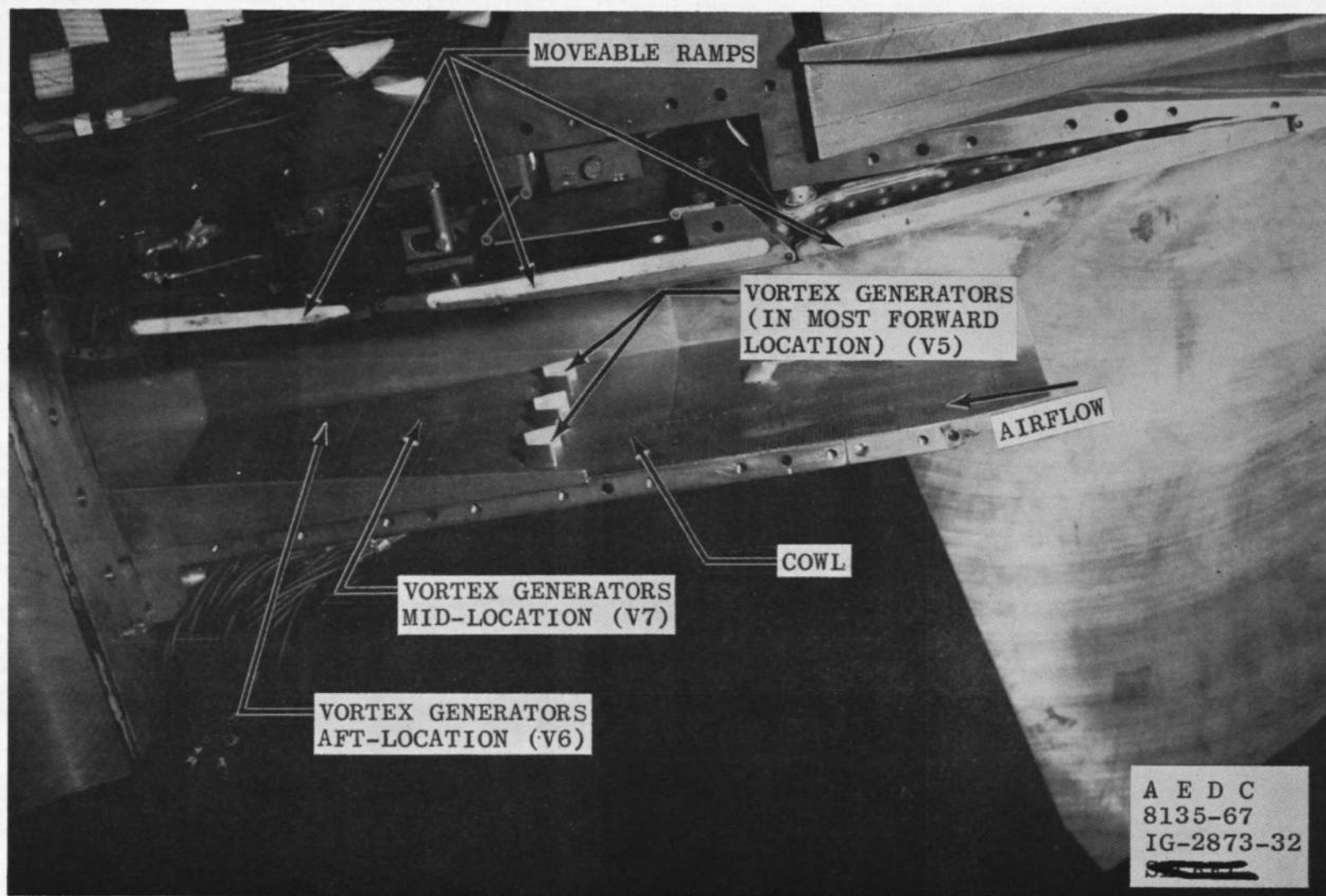
--- ENGINE REQUIREMENT



~~SECRET~~

Fig. 16 Inlet Performance of Subsonic Diffusers A and D as a Function of Mass-Flow Ratio,  $M_\infty = 2.20$ ,  $\alpha = 4.0$  deg,  $\psi = 0$  deg, TH = 110 percent T-L

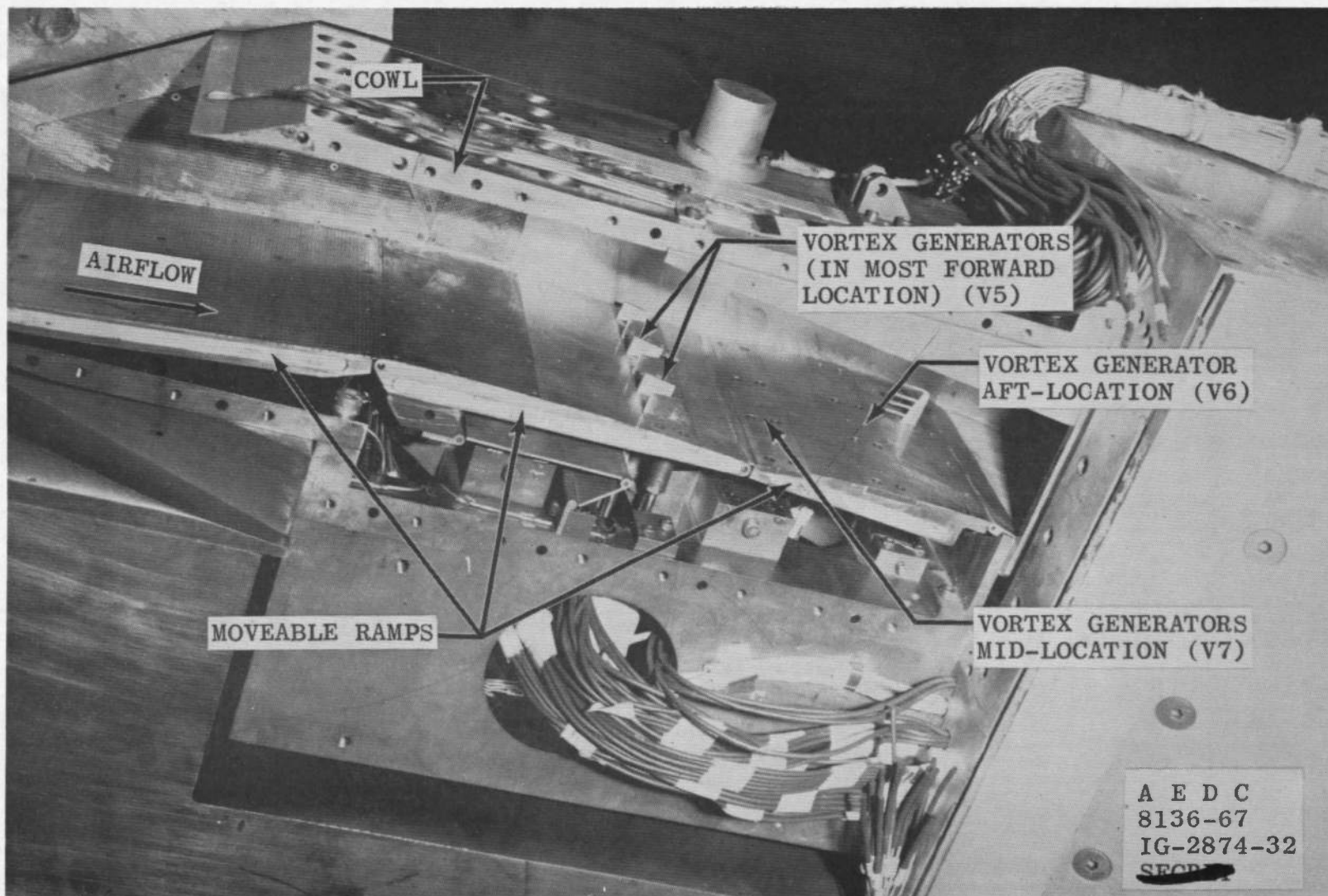
DECLASSIFIED / UNCLASSIFIED



a. Cowl Surface

Fig. 17 (Unclassified) Location of Vortex Generators

DECLASSIFIED / UNCLASSIFIED



b. Ramp Surface  
Fig. 17 Concluded

DECLASSIFIED / UNCLASSIFIED

AEDC-TR-67-213

~~SECRET~~

DECLASSIFIED / UNCLASSIFIED

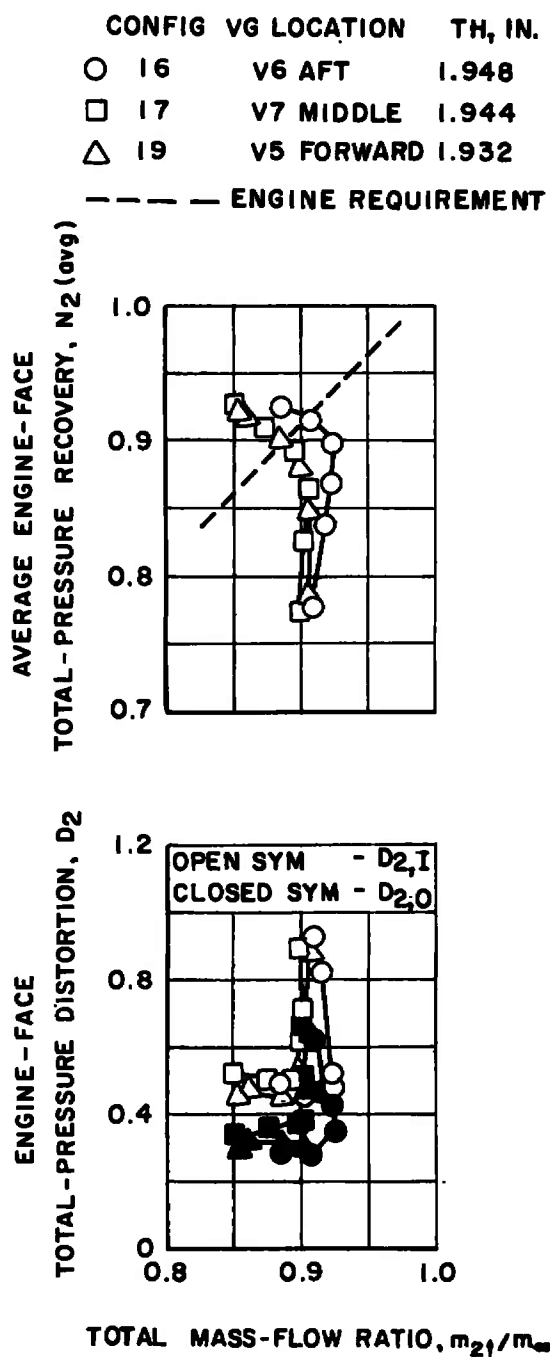


Fig. 18 (Semi) Effect of Vortex Generator Location on Inlet Performance,  $M_\infty = 2.20$ ,  $\alpha = 4.0$  deg,  $\psi = 0$  deg, TH = 104 percent T-L

DECLASSIFIED / UNCLASSIFIED

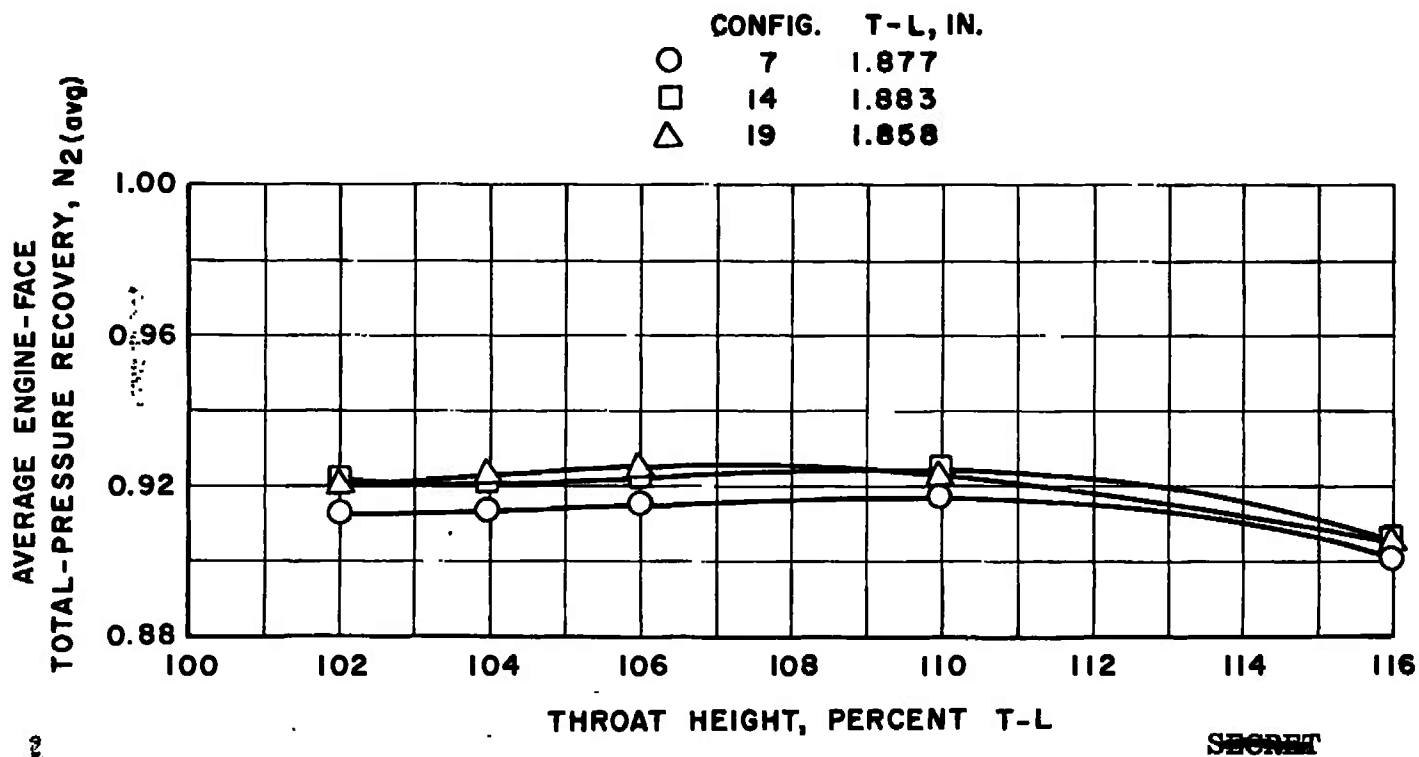


Fig. 19 (~~Secret~~) Variation in Total-Pressure Recovery as a Function  
 of Throat Height for Model Configurations 7, 14, and 19,  
 $M_\infty = 2.20$ ,  $\alpha = 4.0$  deg,  $\psi = 0$  deg

~~SECRET~~

DECLASSIFIED / UNCLASSIFIED

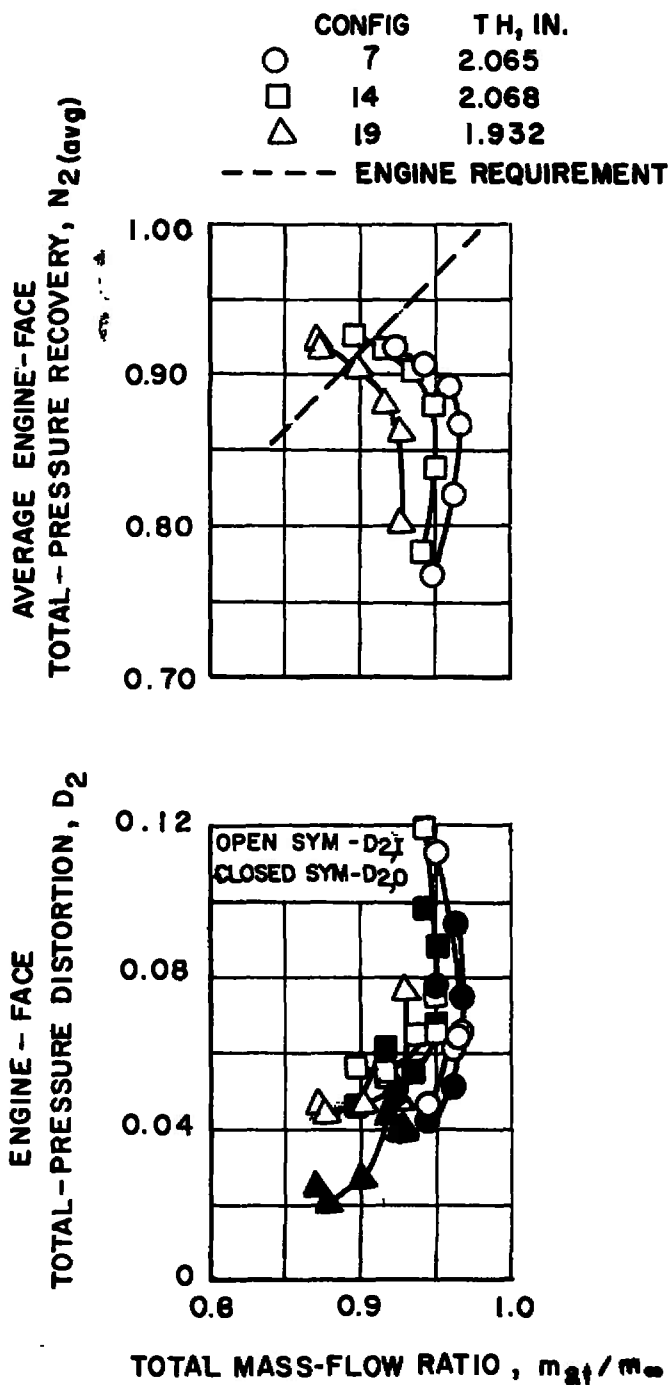
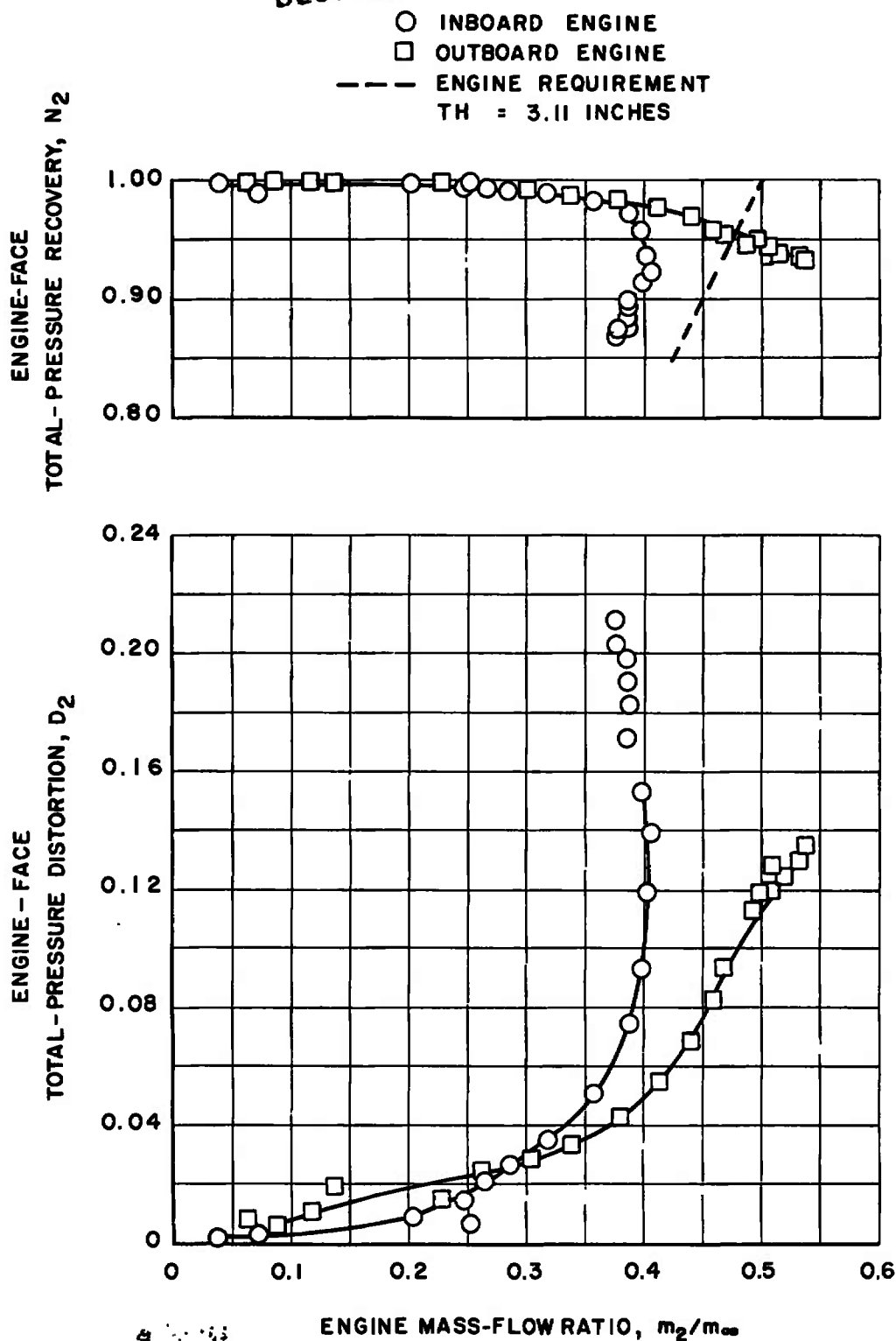
~~SECRET~~

Fig. 20 (~~SECRET~~) Inlet Performance of Model Configurations 7, 14, and 19 as a Function of Total Engine Mass-Flow Ratio,  $M_{\infty} = 2.20$ ,  $\alpha = 4.0$  deg,  $\psi = 0$  deg, TH = 110 percent T-L

DECLASSIFIED / UNCLASSIFIED

~~SECRET~~

DECLASSIFIED / UNCLASSIFIED

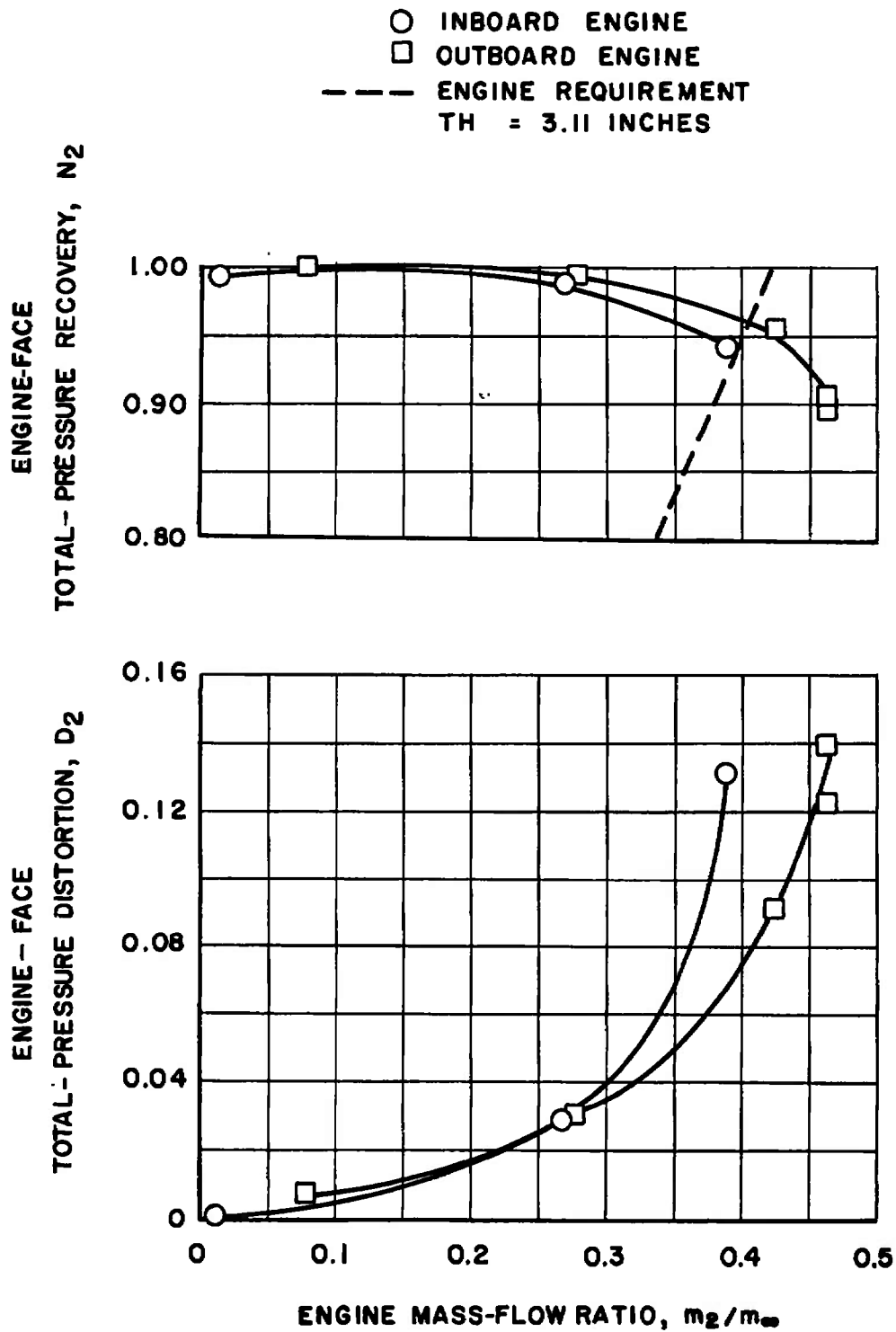


~~SECRET~~

a.  $M_\infty = 0.60$ , Configuration 22

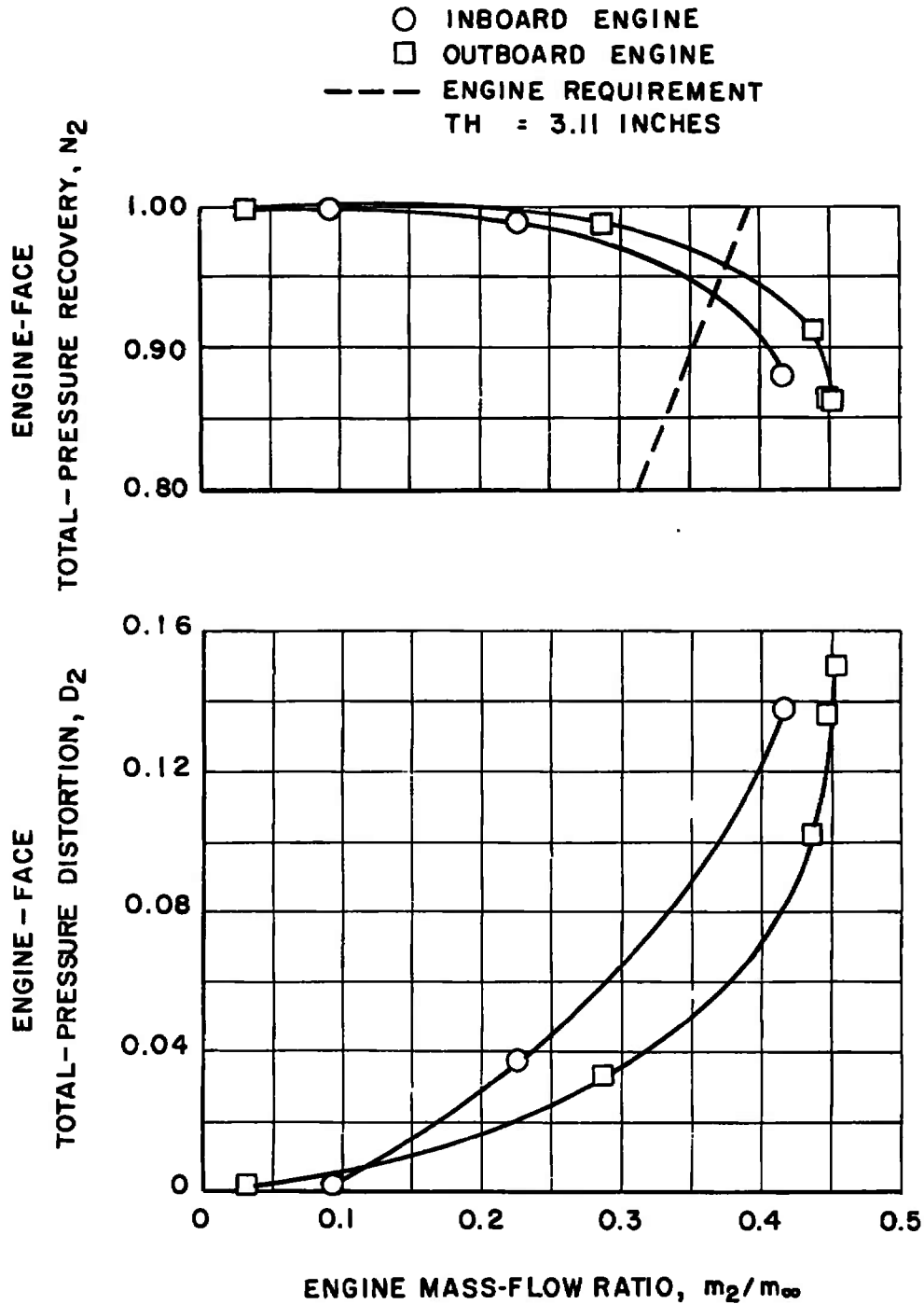
Fig. 21 Effect of Mach Number on Inlet Performance,  $\alpha = 4.0$  deg,  $\psi = 0$  deg

DECLASSIFIED / UNCLASSIFIED



b.  $M_\infty = 0.85$ , Configuration 22

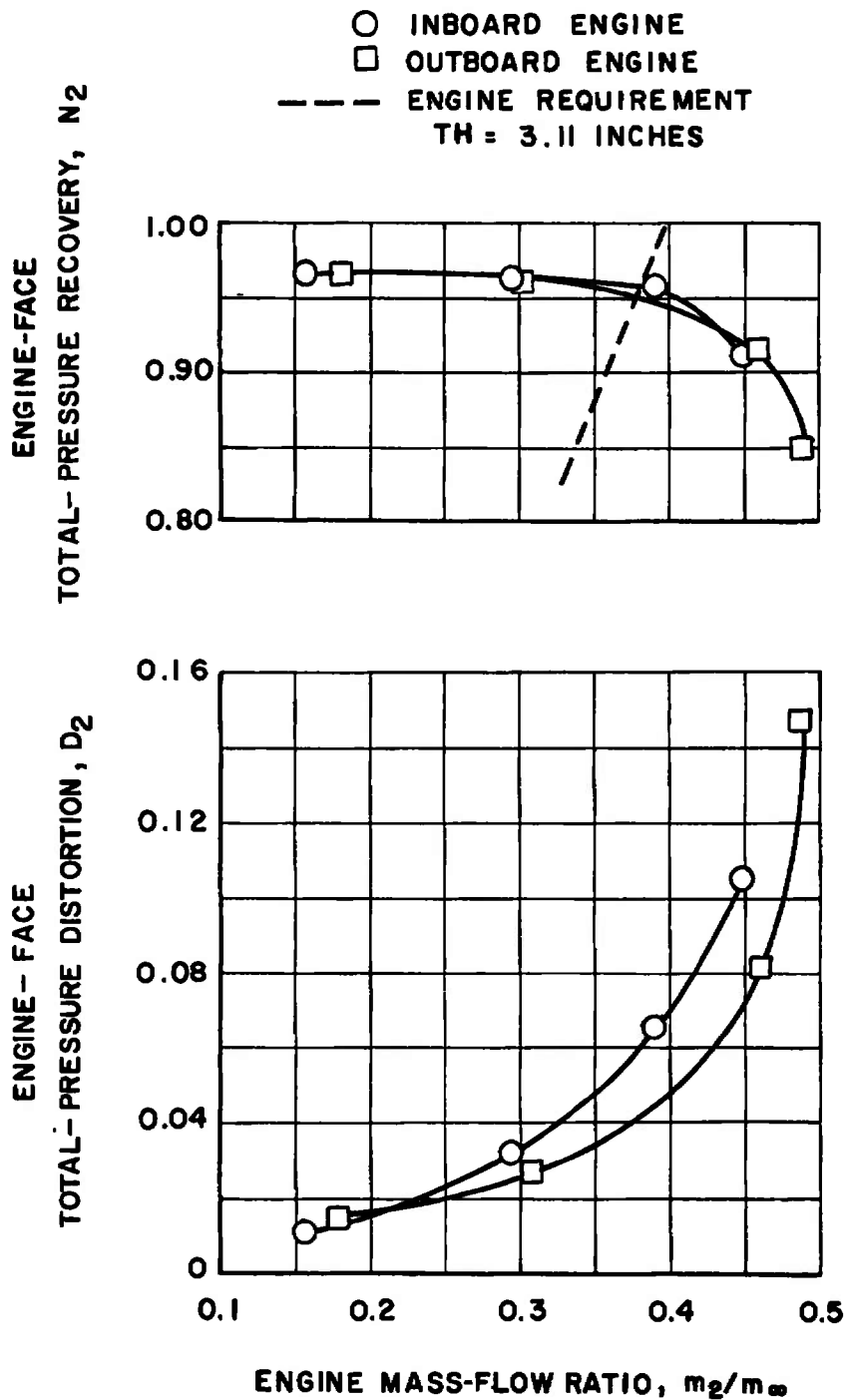
Fig. 21 Continued



c.  $M_\infty = 1.20$ , Configuration 22

Fig. 21 Continued

~~SECRET~~  
DECLASSIFIED / UNCLASSIFIED



~~SECRET~~  
d.  $M_\infty = 1.50$ , Configuration 27

Fig. 21 Continued

DECLASSIFIED / UNCLASSIFIED

~~SECRET~~  
DECLASSIFIED / UNCLASSIFIED

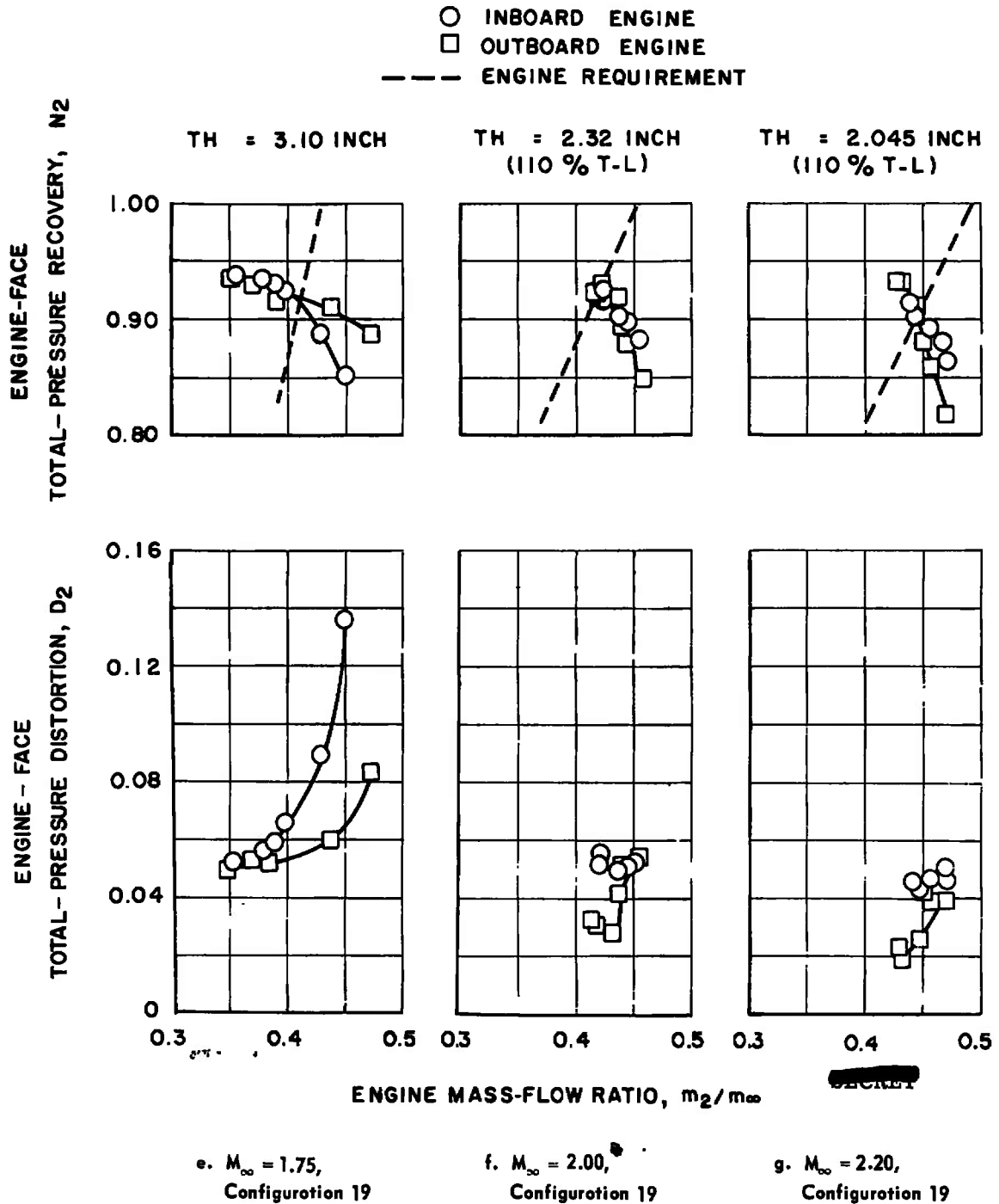
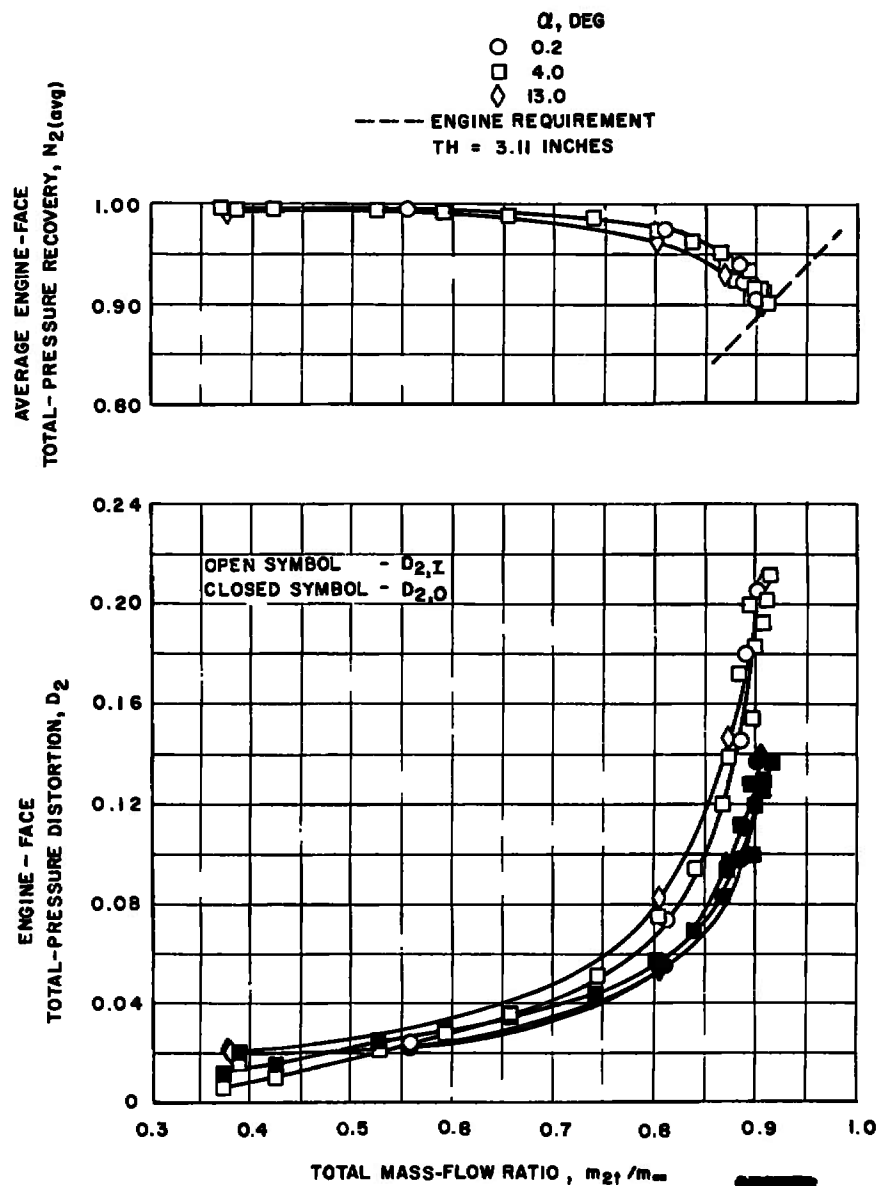


Fig. 21 Concluded

~~SECRET~~  
DECLASSIFIED / UNCLASSIFIED

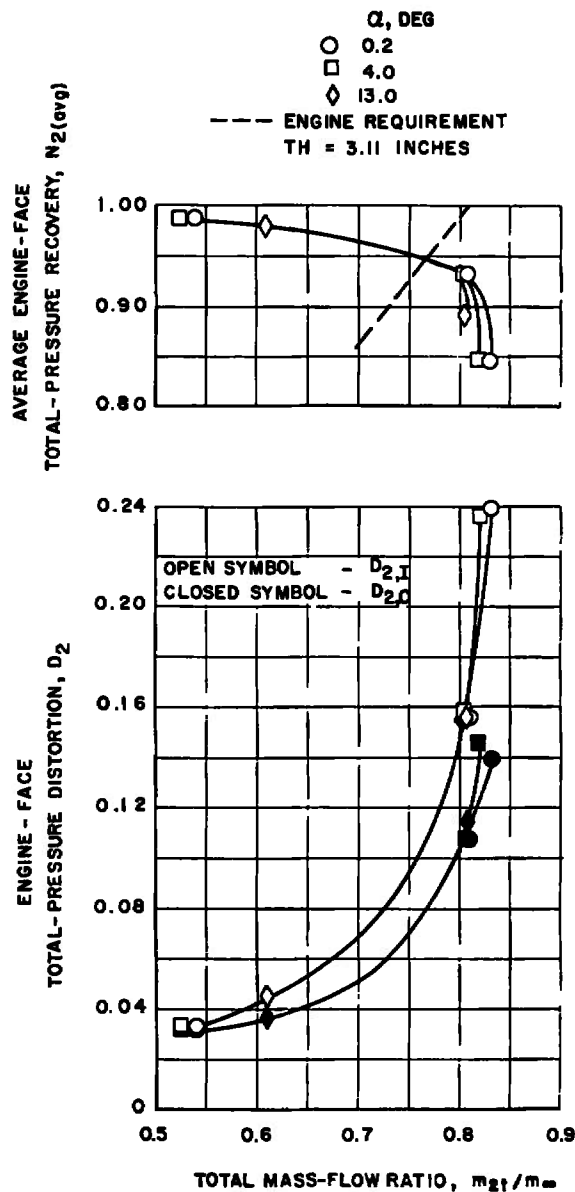
DECLASSIFIED / UNCLASSIFIED

a.  $M_{\infty} = 0.60$ , Configuration 22Fig. 22 (Semi) Effect of Attack on Inlet Performance,  $\psi = 0$  deg

DECLASSIFIED / UNCLASSIFIED

**SECRET**

DECLASSIFIED / UNCLASSIFIED



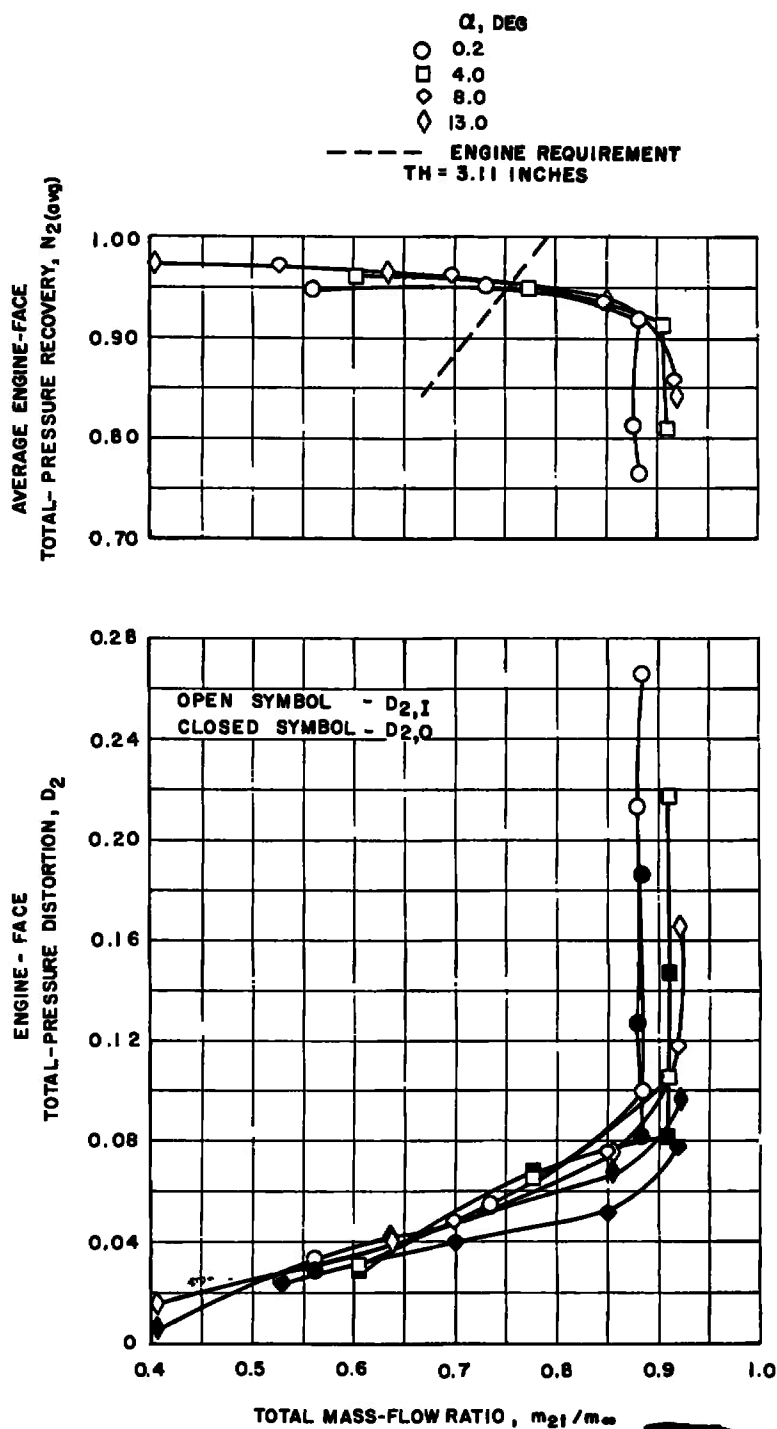
b.  $M_{oc} = 0.95$ , Configuration 22

Fig. 22 Continued

**SECRET**

DECLASSIFIED / UNCLASSIFIED

**SECRET**  
 DECLASSIFIED / UNCLASSIFIED

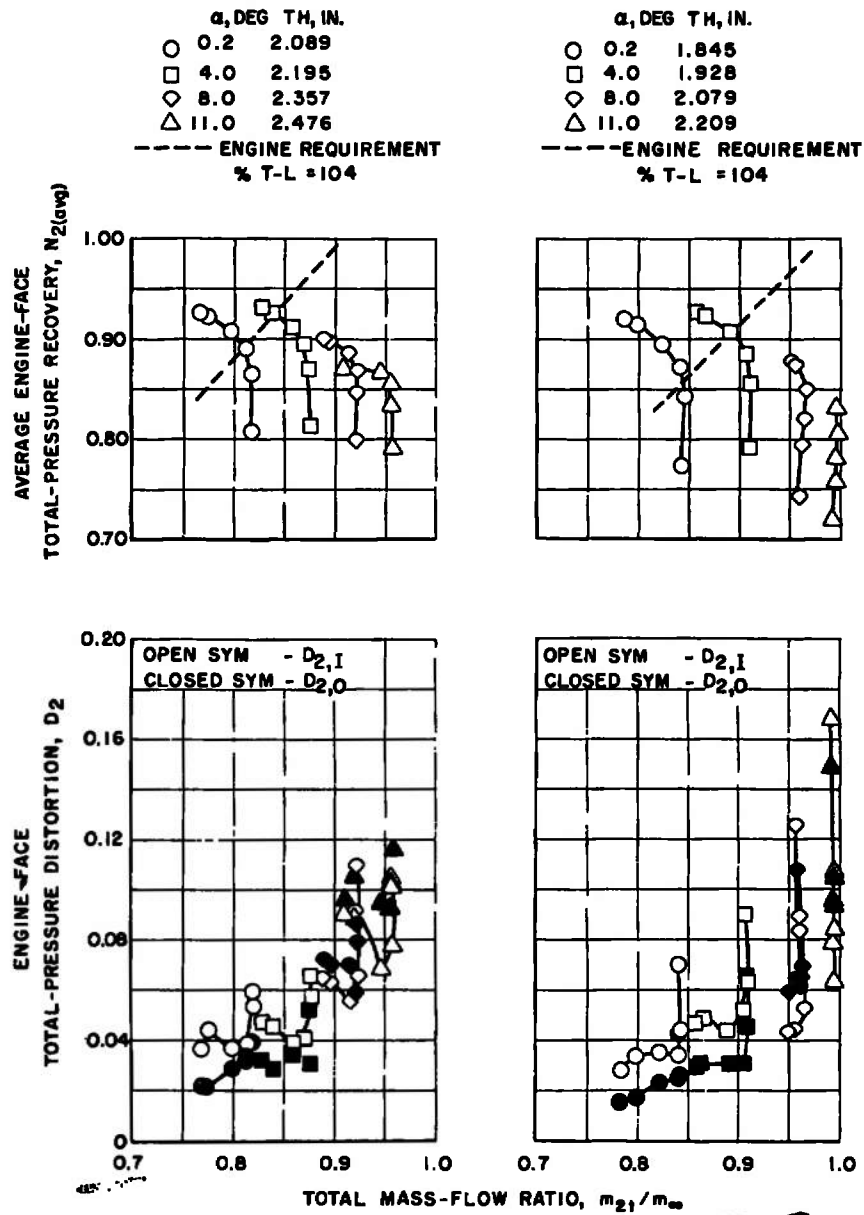


c.  $M_{\infty} = 1.50$ , Configuration 27

Fig. 22 Continued

**SECRET**  
 DECLASSIFIED / UNCLASSIFIED

DECLASSIFIED / UNCLASSIFIED



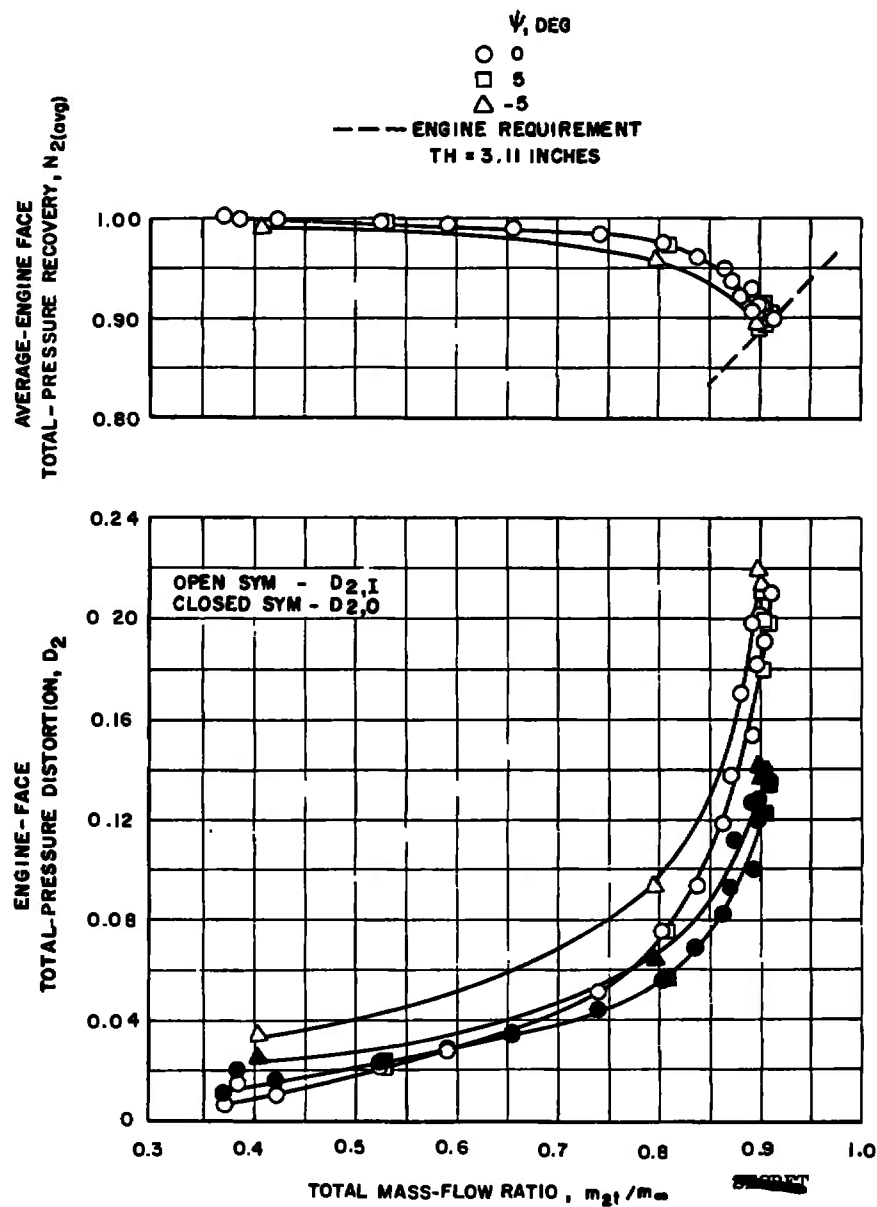
SECRET

d.  $M_\infty = 2.00$ , Configuration 19e.  $M_\infty = 2.20$ , Configuration 19

Fig. 22 Concluded

DECLASSIFIED / UNCLASSIFIED

DECLASSIFIED / UNCLASSIFIED

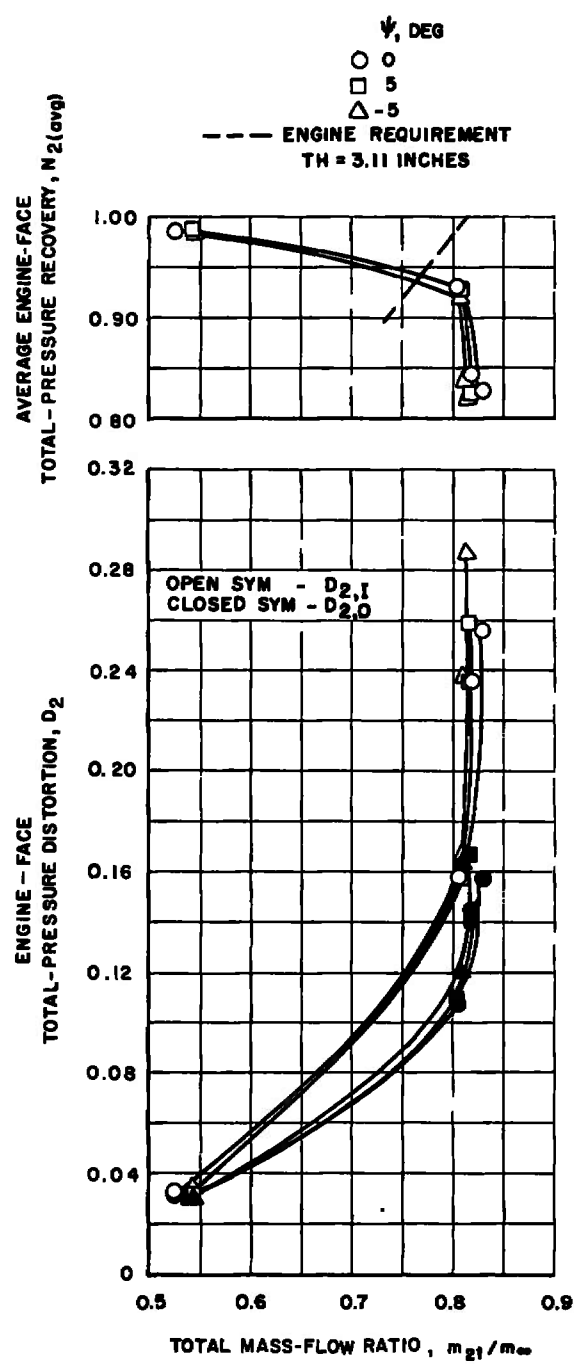


a.  $M_{\infty} = 0.60$ , Configuration 22

Fig. 23 Effect of Yaw on Inlet Performance,  
 $\alpha = 4.0$  deg,  $\psi = -5.0$  to  $+5.0$  deg

DECLASSIFIED / UNCLASSIFIED

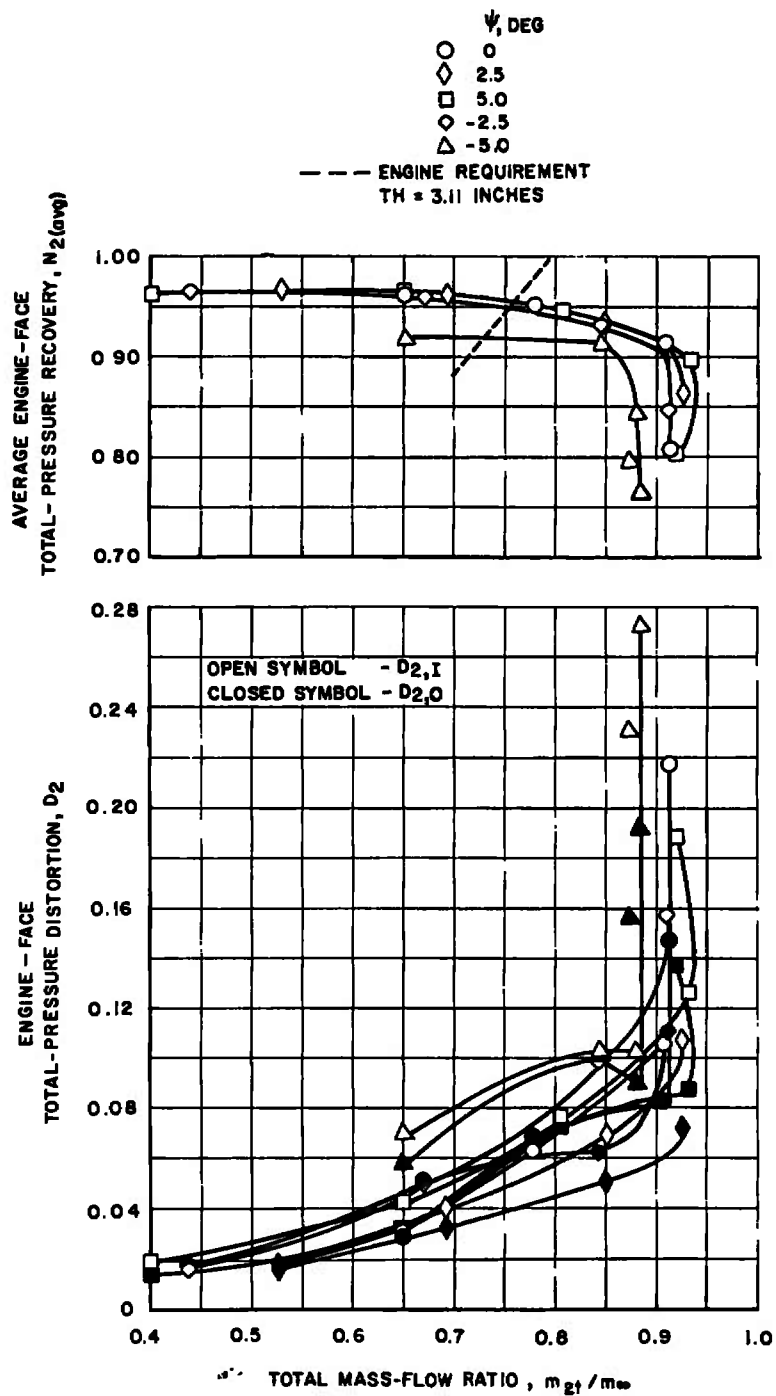
DECLASSIFIED / UNCLASSIFIED



b.  $M_{\infty} = 0.95$ , Configuration 22

Fig. 23 Continued

DECLASSIFIED / UNCLASSIFIED

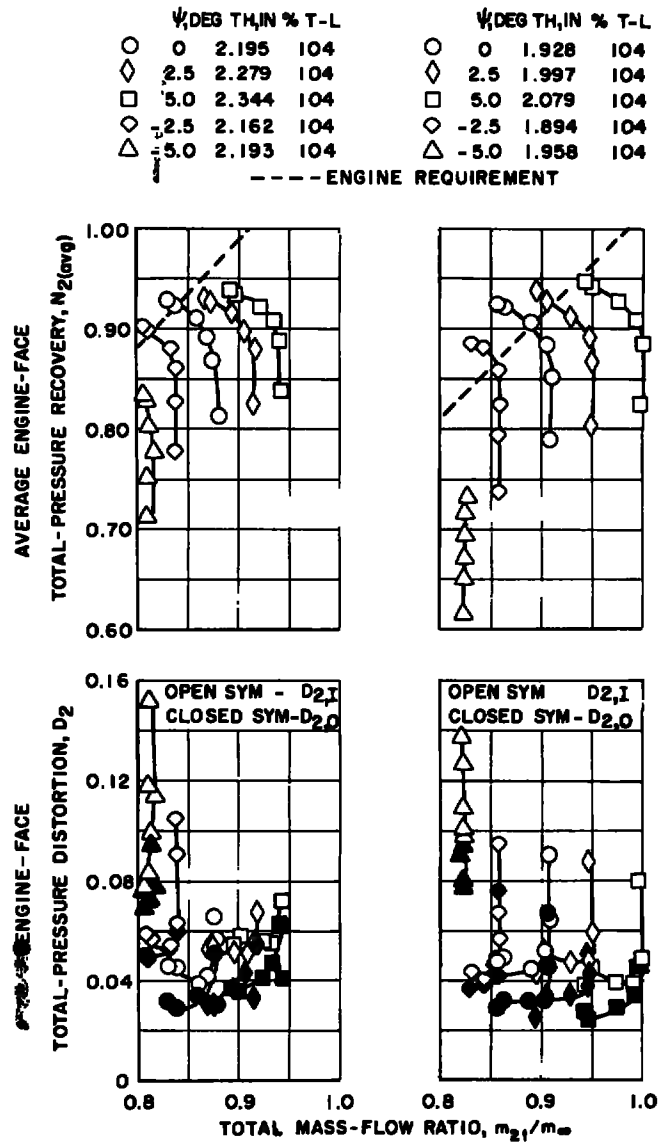


c.  $M_{\infty} = 1.50$ , Configuration 27

Fig. 23 Continued

DECLASSIFIED / UNCLASSIFIED

**DECLASSIFIED / UNCLASSIFIED**



d.  $M_{\infty} = 2.00$ ,  
Configuration 19

e.  $M_{\infty} = 2.20$ ,  
Configuration 19

Fig. 23 Concluded

DECLASSIFIED / UNCLASSIFIED

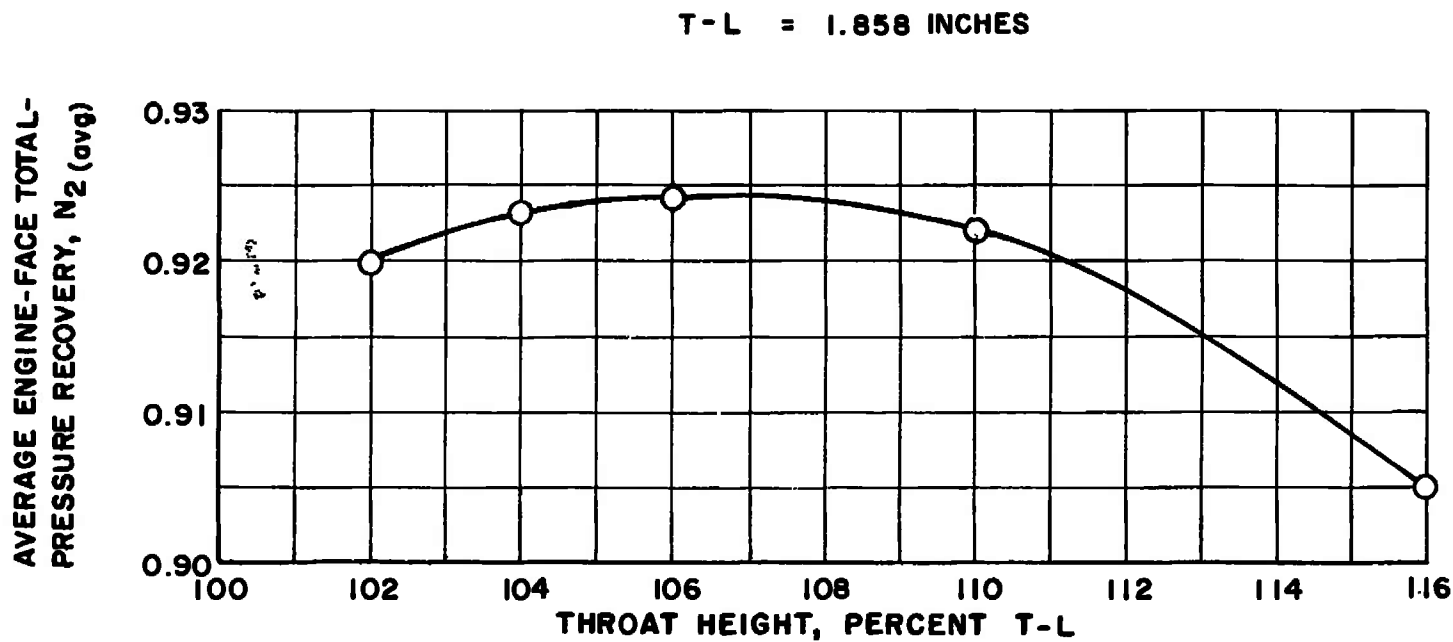
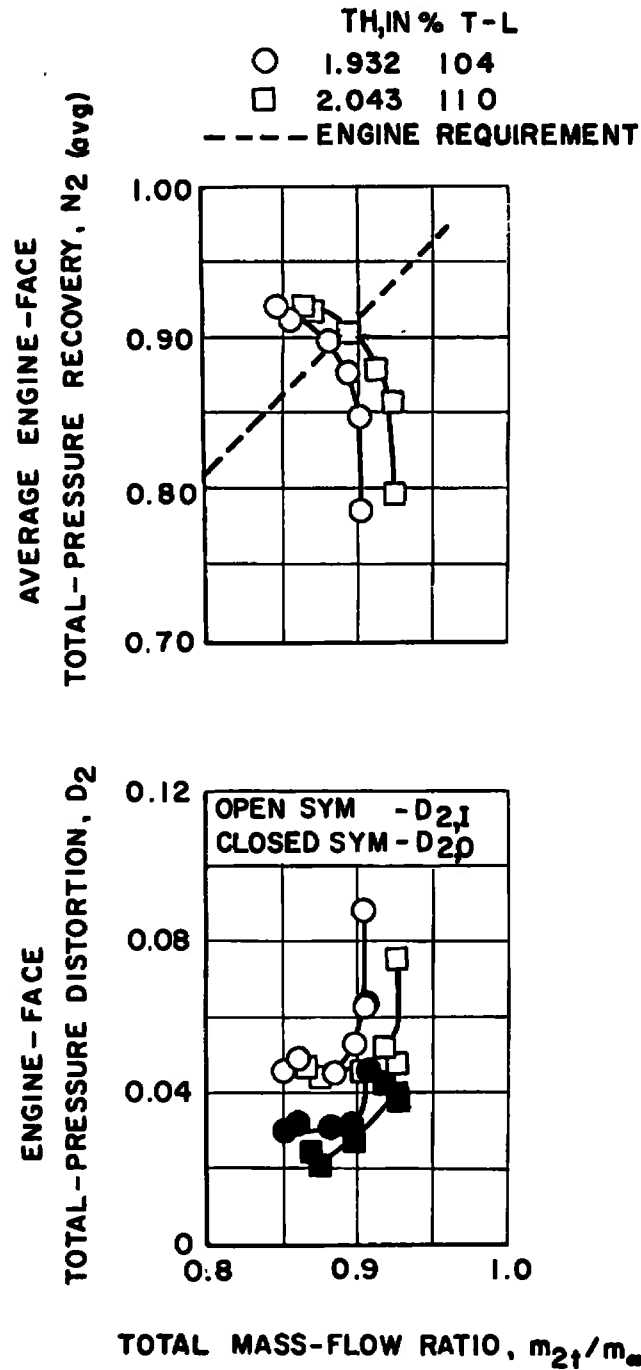
~~SECRET~~

Fig. 24 ~~(SECRET)~~ Variation of Total-Pressure Recovery as a Function of Throat Height,  
 $M_{\infty} = 2.20$ ,  $\alpha = 4.0$  deg,  $\psi = 0$  deg, Configuration 19

DECLASSIFIED / UNCLASSIFIED

SECRET  
DECLASSIFIED / UNCLASSIFIED

AEDC-TR-67-213



SECRET

a.  $M_{\infty} = 2.20$

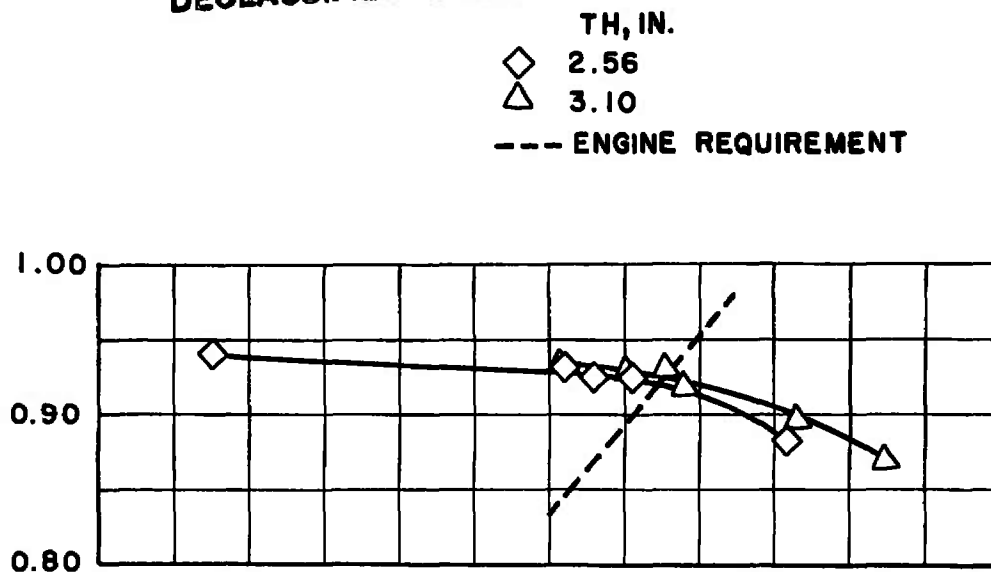
Fig. 25 Effect of Throat Height on Inlet Performance,  
 $\alpha = 4.0$  deg,  $\psi = 0$  deg, Configuration 19

DECLASSIFIED / UNCLASSIFIED

~~SECRET~~

DECLASSIFIED / UNCLASSIFIED

AVERAGE ENGINE-FACE  
TOTAL-PRESSURE RECOVERY,  $N_2$  (avg)



ENGINE-FACE  
TOTAL-PRESSURE DISTORTION,  $D_2$

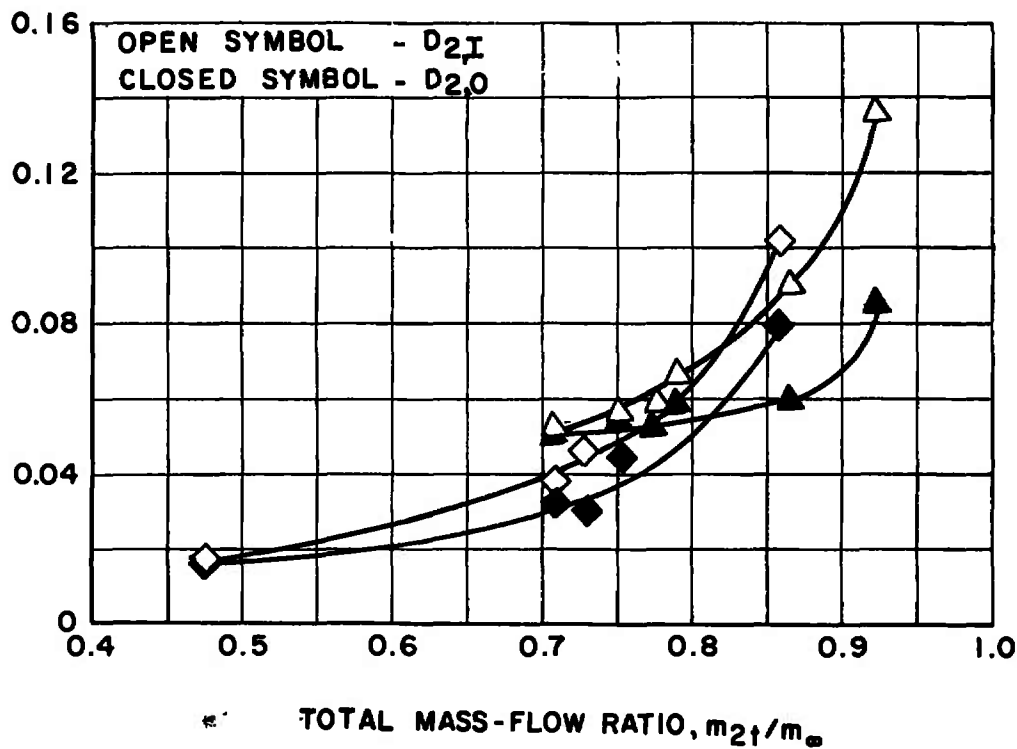
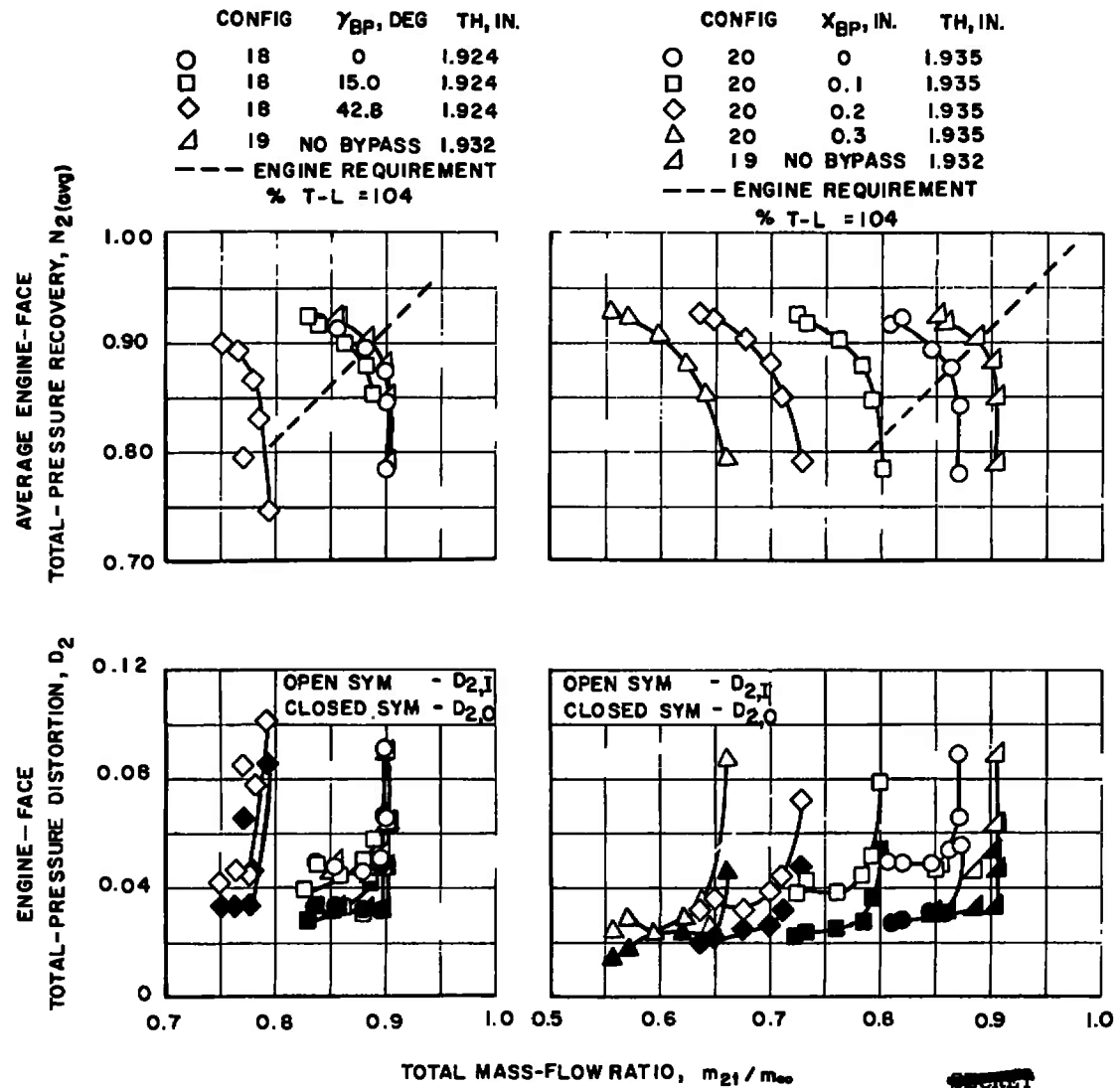
TOTAL MASS-FLOW RATIO,  $m_{2t}/m_\infty$ ~~SECRET~~b.  $M_\infty = 1.75$ 

Fig. 25 Concluded

DECLASSIFIED / UNCLASSIFIED

~~SECRET~~

DECLASSIFIED / UNCLASSIFIED



a. Bypass Configuration U1

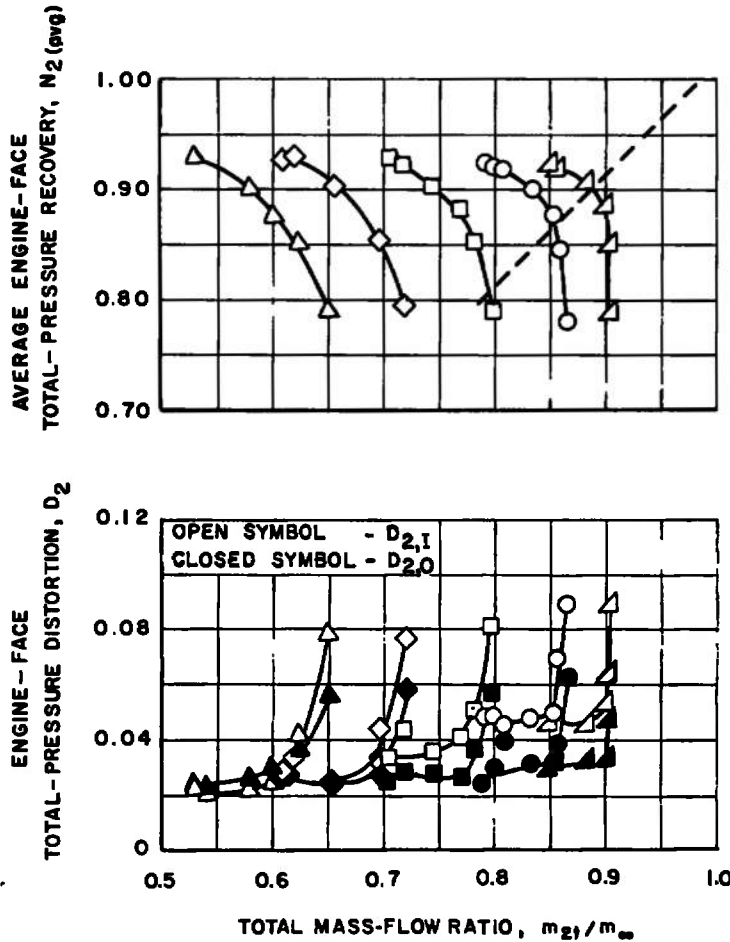
b. Bypass Configuration U3

Fig. 26 (SECRET) Effect of Bypass Configuration on Inlet Performance,  
 $M_{\infty} = 2.20$ ,  $\alpha = 4.0$  deg,  $\psi = 0$  deg

DECLASSIFIED / UNCLASSIFIED

DECLASSIFIED / UNCLASSIFIED

	CONFIG.	$X_{BP}, \text{IN.}$	$T_H, \text{IN.}$
○	21	0.0	1.935
□	21	0.1	1.935
◇	21	0.2	1.935
△	21	0.3	1.935
▴	19	NO BYPASS	1.932
--- ENGINE REQUIREMENT			
% T-L = 104			



c. Bypass Configuration U2  
Fig. 26 Concluded

DECLASSIFIED / UNCLASSIFIED

**TABLE I**  
**CONFIGURATION DESCRIPTION**

Config. No.	Fuse-lage	Fuselage Inlet B/L Gutter	Wing	Wing Inlet B/L Gutter	Subsonic Diffuser	B/L Bleed Pattern	Cowl	Vortex Generator Config.	Bypass Config.	Metering Main Duct Config.
1	B1	FG1	W1	WG1	I1(A)	J1	L0	VO	U0	M1
2	↓	FG2	↓	↓	↓	J2	↓	↓	↓	↓
3	↓	↓	↓	↓	↓	J3	↓	↓	↓	↓
4	↓	↓	↓	↓	↓	J4	↓	↓	↓	↓
5	↓	↓	↓	↓	↓	J1	↓	↓	↓	↓
6	↓	↓	↓	↓	↓	J4	↓	↓	↓	↓
7	↓	↓	↓	↓	I2(D)	↓	↓	↓	↓	↓
8	↓	↓	↓	↓	I4(G)	↓	↓	↓	↓	↓
9	↓	↓	↓	↓	I3(F)	↓	↓	↓	↓	↓
10	↓	↓	↓	↓	I3(F)	J5	↓	↓	↓	↓
11	↓	↓	↓	↓	I2(D)	J6	↓	↓	↓	↓
12	↓	↓	↓	↓	↓	J6	↓	↓	↓	↓
13	↓	↓	↓	↓	↓	J7	↓	↓	↓	↓
14	↓	↓	↓	↓	↓	J8	↓	↓	↓	↓
15	↓	↓	↓	↓	↓	↓	↓	V5	↓	↓
16	↓	↓	↓	↓	↓	↓	↓	V6	↓	↓
17	↓	↓	↓	↓	↓	↓	↓	V7	↓	↓
18	↓	↓	↓	↓	↓	↓	↓	V5	↓	↓
19	↓	↓	↓	↓	↓	↓	↓	↓	U1	↓
20	↓	↓	↓	↓	↓	↓	↓	↓	U0	↓
21	↓	↓	↓	↓	↓	↓	↓	↓	U3	↓
22	↓	↓	↓	↓	↓	↓	↓	↓	U2	↓
23	↓	↓	↓	↓	↓	J9	L1	↓	U0	↓
24	↓	↓	↓	↓	↓	J8	L0	↓	U0	↓
25	↓	↓	↓	↓	↓	↓	↓	↓	U3	↓
26	↓	↓	↓	↓	I1(A)	↓	↓	↓	U2	↓
27 *	↓	↓	↓	↓	I2(D)	↓	↓	↓	U0	↓

\*Same as 22

~~SECRET~~

DECLASSIFIED / UNCLASSIFIED

DECLASSIFIED / UNCLASSIFIED

~~SECRET~~

## DECLASSIFIED / UNCLASSIFIED

## APPENDIX III

## THE INFLUENCE OF THE MODEL SUPPORT STRUCTURE ON THE FLOW ANGULARITY AND LOCAL MACH NUMBER AT TRANSONIC MACH NUMBERS

(Unclassified) An investigation was conducted in Tunnel 16T to determine the influence of the model support structure on the flow angularity and local Mach number in the model inlet flow field. The model was removed from the support for this study to test the effect of the support alone (Fig. III-1). A hemispherical differential pressure yawmeter probe was mounted on the support such that the flow conditions at the model inlet location were determined. The yawmeter probe was also equipped with a pitot orifice and with static orifices for determining local Mach number. The model support was found to exert a strong influence on the flow angularity and local Mach number at high subsonic and low transonic speeds. A summary of the flow angularity and Mach number effects is shown in Table III-1. The values for  $\Delta\alpha$  and  $\Delta\psi$  include the tunnel flow misalignment as well as the interference effects caused by the model support structure.

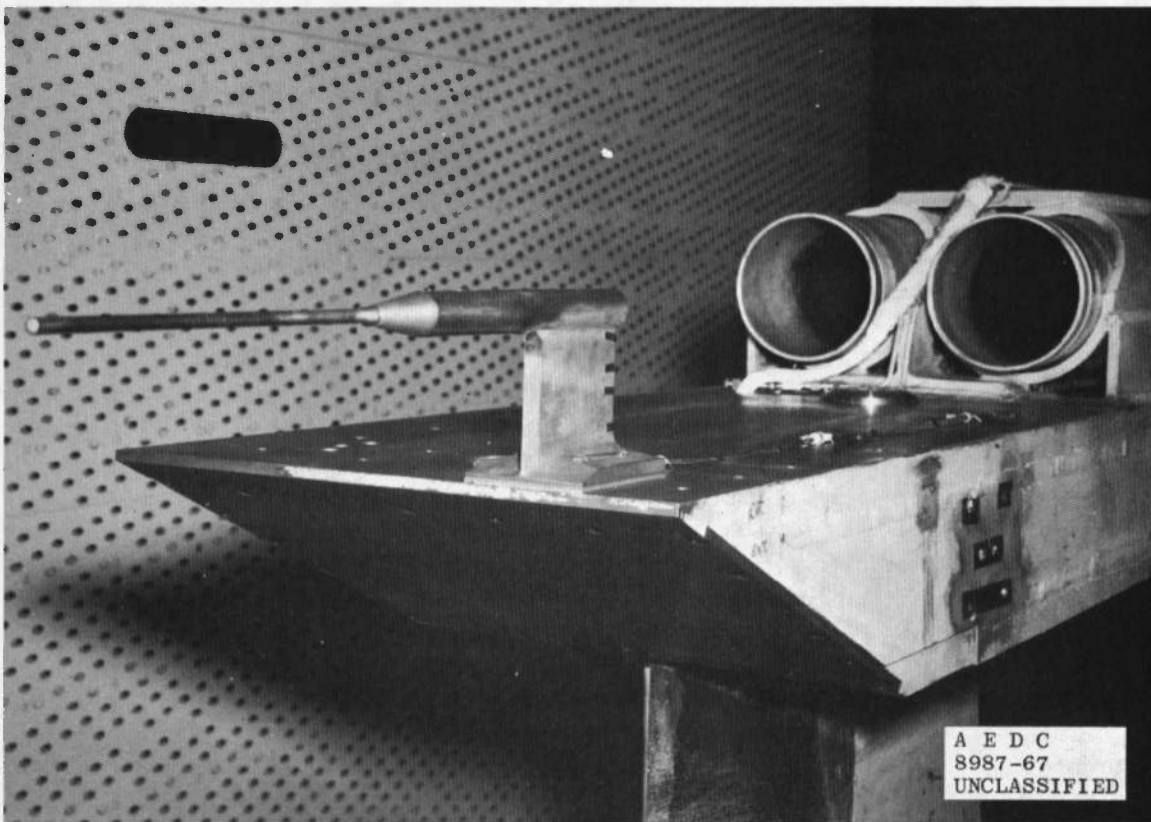


Fig. III-1 Hemispherical Yawmeter on Model Support Structure

62 DECLASSIFIED / UNCLASSIFIED

~~SECRET~~

This page is Unclassified

TABLE III-1  
SUMMARY OF INTERFERENCE EFFECTS

$M_\infty$	$\alpha$	$\psi$	$\Delta M$	$\Delta \alpha$	$\Delta \psi$
0.60	0	0	-0.030	1.24	-0.50
	4	0	-0.035	1.12	-0.50
	8	0	-0.040	0.73	-0.53
	10	0	-0.055	0.46	-0.44
	4	+5	-0.030	1.13	-0.38
	4	-5	-0.025	0.90	-0.30
0.85	0	0	-0.075	0.99	-0.28
	4	0	-0.085	1.15	-0.30
	8	0	-0.100	1.19	-0.49
	10	0	-0.105	1.30	-0.43
	4	+5	-0.092	1.30	-0.20
	4	-5	-0.080	1.03	-0.20
0.95	0	0	-0.118	0.98	-0.30
	4	0	-0.120	1.09	-0.41
	8	0	-0.145	1.36	-0.46
	10	0	-0.150	1.61	-0.59
	4	+5	-0.125	1.25	-0.25
	4	-5	-0.120	1.00	-0.30
1.20	0	0	-0.005	0.23	-0.01
	4	0	-0.010	0.32	-0.08
	8	0	-0.010	0.46	-0.05
	10	0	0	0.76	0
	4	+5	0.010	0.43	0.55
	4	-5	0.010	0.30	0.43
1.50	0	0	0.008	0.34	-0.15
	4	0	0.021	0.17	-0.15
	8	0	0.025	0.28	-0.12
	10	0	0.020	0.19	-0.16
	4	+5	0.045	0.38	0.10
	4	-5	0.055	0	0

UNCLASSIFIED

Security Classification

## DOCUMENT CONTROL DATA - R &amp; D

(Security classification of title, body of abstract and indexing annotation must be entered when the overall report is classified)

1. ORIGINATING ACTIVITY (Corporate author) Arnold Engineering Development Center ARO, Inc., Operating Contractor Arnold Air Force Station, Tennessee		2a. REPORT SECURITY CLASSIFICATION <del>SECRET</del>
		2b. GROUP 3
3. REPORT TITLE WIND TUNNEL INVESTIGATION OF A 0.10-SCALE NORTH AMERICAN AVIATION AMSA INLET AT TRANSONIC AND SUPERSONIC MACH NUMBERS (U)		
4. DESCRIPTIVE NOTES (Type of report and inclusive dates) Final Report - May 2-10 and June 2-24, 1967		
5. AUTHOR(S) (First name, middle initial, last name) H. E. McDill and J. F. Riddell, ARO, Inc.		
6. REPORT DATE October 1967	7a. TOTAL NO. OF PAGES 76	7b. NO. OF REFS 3
8a. CONTRACT OR GRANT NO. AF40(600)-1200	9a. ORIGINATOR'S REPORT NUMBER(S) AEDC-TR-67-213	
b. PROJECT NO. c. Program Element 6340683F d. System 139A	9b. OTHER REPORT NO(S) (Any other numbers that may be assigned this report) N/A	
10. DISTRIBUTION STATEMENT Subject to special export controls, transmittal to foreign governments or foreign nationals requires approval of ASD (ASZD), Wright-Patterson AFB, Ohio. In addition, to security requirements which apply to this document and must be met, each transmittal outside the*		
11a. SUPPLEMENTARY NOTES Available in DDC.	12. SPONSORING MILITARY ACTIVITY Aeronautical Systems Division (ASZD) Air Force Systems Command, Wright-Patterson AFB, Ohio	
13. ABSTRACT  Test results are presented for a study on a 0.10-scale model of the North American Aviation proposed advanced manned strategic aircraft air vehicle. Inlets of various geometries were tested at several Mach numbers, angles of attack, and angles of yaw. Inlet performance in terms of compressor face total-pressure recovery and flow distortion is presented as a function of mass-flow ratio for various inlet geometries at several Mach numbers and model attitudes. (U)  Subject: Distribution limited to U. S. Gov't Agencies only; Test and evaluation; Nov. 72. Other requests for this document must be referred to Commander, Aeronautical Systems Div., Attn: YHT, Wright-Patterson AFB, Ohio 45433. Per TAB 73, dated 15 Jan. 73.  * Department of Defense must have prior approval of Aeronautical Systems Division (ASZD), Wright-Patterson AFB, Ohio.		

14.	KEY WORDS	LINK A		LINK B		LINK C	
		ROLE	WT	ROLE	WT	ROLE	WT
	air inlets wind tunnel tests AMSA performance operating characteristics angle of attack angle of yaw						
	1. Air inlets -- Performance 2 Airplanes -- AMSA						
	1 - 2						